J|A|C|S

JOURNAL OF THE AMERICAN CHEMICAL SOCIETY

Article

An Improved P^{III}/P^V=O-Catalyzed Reductive C−N Coupling of Nitroaromatics and Boronic Acids by Mechanistic Differentiation of Rate- and Product-Determining Steps

Gen Li, Trevor V. Nykaza, Julian C. Cooper, Antonio Ramirez, Michael R. Luzung, and Alexander T. Radosevich*

Read Online

ACCESS | Metrics & More | Article Recommendations | SI Supporting Information

ABSTRACT: Experimental, spectroscopic, and computational studies are reported that provide an evidence-based mechanistic description of an intermolecular reductive C−N coupling of nitroarenes and arylboronic acids catalyzed by a redox-active main-group catalyst (1,2,2,3,4,4-hexamethylphosphetane *P*-oxide, i.e., 1·[O]). The central observations include the following: (1) catalytic reduction of 1·[O] to P^{III} phosphetane 1 is kinetically fast under conditions of catalysis; (2) phosphetane 1 represents the catalytic resting state as observed by ^{31}P NMR spectroscopy; (3) there are no long-lived nitroarene partial-reduction intermediates observable by ^{15}N NMR spectroscopy; (4) the reaction is sensitive to solvent dielectric, performing best in moderately polar solvents (viz. cyclopentylmethyl ether); and (5) the reaction is largely insensitive with respect to common hydrosilane reductants. On the basis of the foregoing studies, new modified catalytic conditions are described that expand the reaction scope and provide for mild temperatures ($T \geq 60$ °C), low catalyst loadings (≥ 2 mol%), and innocuous terminal reductants (polymethylhydrosiloxane). DFT calculations define a two-stage deoxygenation sequence for the reductive C−N coupling. The initial deoxygenation involves a rate-determining step that consists of a (3+1) cheletropic addition between the nitroarene substrate and phosphetane 1; energy decomposition techniques highlight the biphilic character of the phosphetane in this step. Although kinetically invisible, the second deoxygenation stage is implicated as the critical C−N product-forming event, in which a postulated oxazaphosphirane intermediate is diverted from arylnitrene dissociation toward heterolytic ring opening with the arylboronic acid; the resulting dipolar intermediate evolves by antiperiplanar 1,2-migration of the organoboron residue to nitrogen, resulting in displacement of 1·[O] and formation of the target C−N coupling product upon *in situ* hydrolysis. The method thus described constitutes a mechanistically well-defined and operationally robust main-group complement to the current workhorse transition-metal-based methods for catalytic intermolecular C−N coupling.
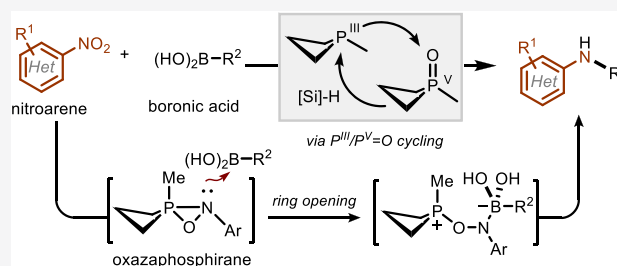
1. INTRODUCTION

Aryl- and heteroarylamines are common in pharmaceuticals, natural products, agrochemicals, and functional materials.[1] Consequently, the efficient construction of C−N bonds has been the target of considerable innovation. In particular, developments in transition-metal-catalyzed C−N coupling chemistry have shaped the dominant approach to arylamine synthesis.[2] Chief among these methods is the Buchwald−Hartwig reaction (Figure 1A),[3] which enables the net *redox-neutral* nucleophilic substitution of aryl (pseudo)halide with N-nucleophiles via Pd(0)/Pd(II) activation of the electrophilic partner through oxidative addition.[4,5] A growing mastery over this important reaction has been enabled by increasingly detailed mechanistic understanding,[6] with progressive optimizations of reaction conditions,[7] ligands,[8] and catalyst precursors[9] resulting in ever-improving scope and efficiency.[10]

In an alternative approach, intermolecular C−N cross coupling can be achieved in an *oxidative* manner by the reaction of N-nucleophiles with arylboron reagents under aerobic copper catalysis (i.e., Chan−Lam reaction, Figure 1B). In addition to the synthetic complementarity, this approach is supported in a practical sense by the impressive catalog of arylboron derivatives now available both commercially and by synthesis.[11] And as with the Buchwald−Hartwig reaction, considerable experimental effort has helped to decrypt significant aspects of the Chan−Lam mechanism,[12] providing the basis for an increasingly reliable and predictive model of reactivity with this method.[13]
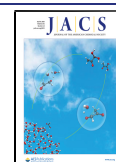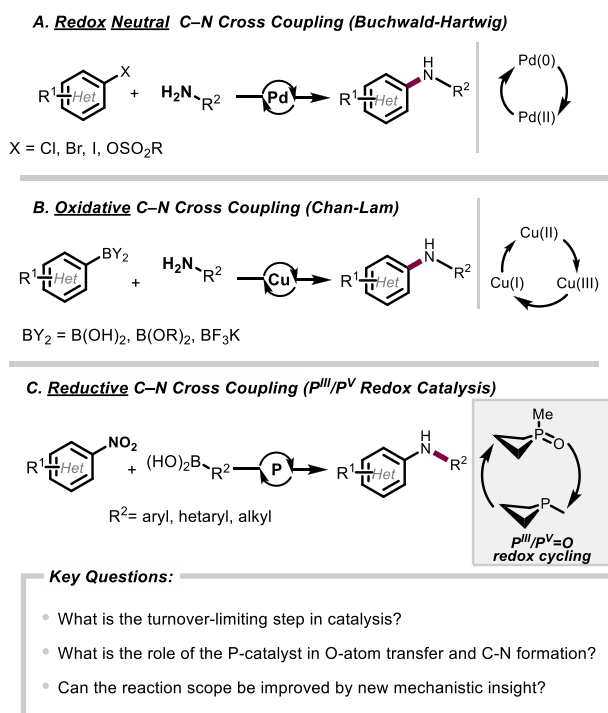
Figure 1. (A) Redox-neutral C−N cross coupling (Buchwald−Hartwig). (B) Oxidative C−N cross coupling (Chan−Lam). (C) Reductive C−N cross coupling (P^{III}/P^{V}=O redox catalysis).

As part of an ongoing program aimed at developing designer main-group compounds as biphilic[14] organocatalysts in organic synthesis,[15] we reported recently a *reductive* method for intermolecular C−N cross coupling. This method relies on an all-main-group system composed of an organophosphorus $P(III)/P(V)$=O redox catalyst and hydrosilane terminal reductant to transform nitroarenes and boronic acids into *N*-arylamines through intermolecular C−N bond formation (Figure 1C).[16] The chief attributes of this method include (1) the use of precursors (i.e., nitroarenes) that are distinct from—but no less accessible than—those used in established C−N cross coupling methods, and (2) unique chemoselectivities and functional group tolerance inherent to the all-main-group conditions of the P^{III}/P^{V}=O catalytic manifold.

To better understand the reductive $P(III)/P(V)$=O-catalyzed C−N bond-forming process and facilitate its further synthetic development, we were animated by several unresolved questions, including the following: (1) What is the nature of the turnover-limiting step in the catalytic C−N coupling reaction, and what is the role of the organophosphorus catalyst in this step? (2) What is the relationship of the catalytic C−N coupling reaction to related methods involving $P(III)/P(V)$=O-catalyzed nitroarene deoxygenation, and to what extent do the reactive intermediates coincide? (3) Can further improvements in reaction scope be attained, especially as informed through hypothesis-based experimentation within a mechanistic rationale?

In this Article, we provide an integrated experimental, spectroscopic, and computational description of the biphilic organophosphorus-catalyzed reductive C−N coupling strategy that systematically delineates the nature of deoxygenative events of nitroaromatics, especially in the context of the C−N bond formation. Among the key findings, we present herein: (1) a qualitative description of reaction parameters, culminat-

ing in a generally improved set of reaction conditions that enable heretofore challenging coupling reactions of azaheterocyclic nitroarene and boronic acids partners; (2) competition experiments that differentiate the intermolecular C−N cross coupling reaction from previous $P(III)/P(V)$=O-catalyzed C−N bond-forming methods, and weigh against the intermediacy of veritable arylnitrene intermediates along the C−N coupling pathway, (3) experimental spectroscopic and kinetic evidence that establish a $P(III)$ resting state of the phosphetane catalyst and imply a rapid $P(V)$=O→$P(III)$ turnover step for this small-ring phosphacycle; (4) a computational description of the overall energy landscape for the C−N coupling reaction pathway with an explicit description of the importance of organophosphorus biphilicity through energy decomposition analysis of the turnover-limiting transition state. Through these results, we establish the $P(III)/P(V)$=O-catalyzed intermolecular reductive C−N cross coupling of nitroarenes and arylboronic acids as an operationally robust and mechanistically well-defined main-group complement to the established transition-metal-based methods for catalytic intermolecular C−N coupling.

2. RESULTS

2.1. Impact of Reaction Condition Variables. An evaluation of experimental variables for the organophosphorus-catalyzed reductive C−N coupling of nitroarenes and boronic acids was undertaken in order to provide a qualitative description of the parameter space that controls reaction yield and efficiency.

2.1.1. Solvent Dielectric Influences Yield. Prior optimization efforts had identified the high-boiling hydrocarbon *m*-xylene (ε = 2.6) as a suitable solvent for reductive intermolecular C−N coupling. Specifically, coupling of nitrobenzene (**2**) and phenylboronic acid (**3**) in *m*-xylene proceeds with full conversion of starting material and an 86% yield of product diphenylamine **4** over the course of 4 h at 120 °C. The ethereal solvent di-*n*-butyl ether (ε = 3.1) performed similarly (Figure 2). However, with increasing solvent polarity a significant and non-monotonic effect of solvent on the reaction outcome was observed. Solvents of moderate polarity, such as cyclopentyl methyl ether (CPME, ε = 4.8) and 1,2-dichlorobenzene (ε = 9.9) lead to improved yields (Table 1, entries 3 and 4), but further increases in solvent polarity (i.e., benzonitrile (PhCN, ε = 26.0), *N*-methyl-2-pyrrolidone (NMP, ε = 32.0), and dimethyl sulfoxide (DMSO, ε = 46.7) were shown to erode both the conversion and the yield. On the basis of the foregoing experiments, CPME—which exhibits favorable process characteristics[17]—was selected as the solvent of choice for the further study.

2.1.2. Performance Is Maintained at Low Catalyst Loading and Temperature. The robustness of the phosphetane catalyst **1**·[O] under conditions of catalysis allow for significant decreases in its loading. For instance, decrease in loading of **1**·[O] to 5 mol% (Table 1, entry 2) or 2 mol% (Table 1, entry 3) permits high conversion and yield, with the provision of a compensatory elongation of the reaction time to 10 and 36 h, respectively. Relatedly, the catalytic transformation is retained with high yield even at temperatures down to 60 °C (Table 1, entries 4 and 5), emphasizing the high reactivity of the phosphetane catalyst.

2.1.3. Numerous Common Hydrosilane Reductants Are Viable. Our "first-generation" conditions for P^{III}/P^{V}=O-catalyzed reductive C−N coupling called for the use of 2.0
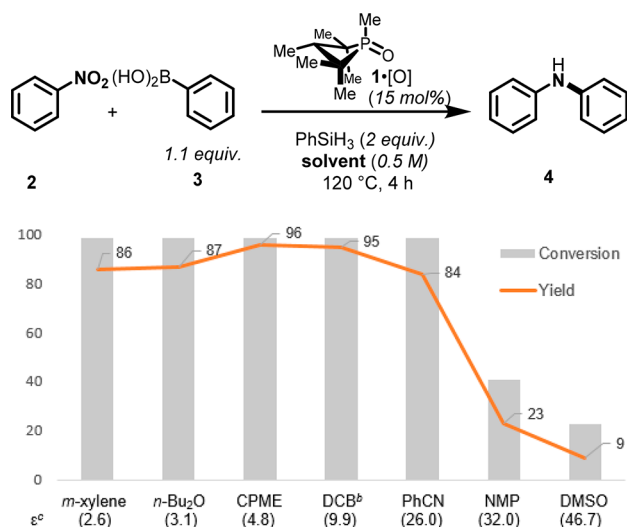
Figure 2. Solvent effect evaluation on the organophosphorus-catalyzed reductive C−N coupling reaction. [a]Yields were determined through analysis by gas chromatography with the use of dodecane as an internal standard. [b]Solvents: CPME, cyclopentyl methyl ether; DCB, 1,2-dichlorobenzene; PhCN, benzonitrile; NMP, N-methyl-2-pyrrolidone; DMSO, dimethyl sulfoxide. [c]ε is the dielectric constant.

Table 1. Effect of Hydrosilane Loading and Identity on the Organophosphorus-Catalyzed Reductive C−N Coupling Reaction

"standard conditions"
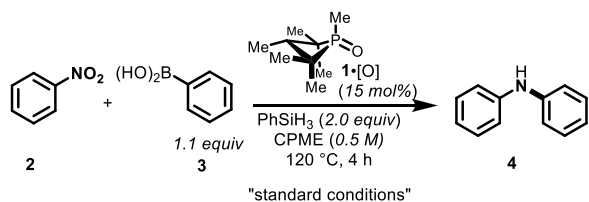
entry	change from "standard conditions"	conv (yield) (%)[a]
1	none	99 (96)
2	5 mol% of 1·[O], 10 h	99 (95)
3	2 mol% of 1·[O], 36 h	99 (93)
4	80 °C, 20 h	99 (95)
5	60 °C, 96 h	99 (93)
6	0.77 equiv of PhSiH₃	98 (94)
7	0.66 equiv of PhSiH₃	85 (79)
8	0.33 equiv of PhSiH₃	49 (46)
9	3.0 equiv of Ph₂SiH₂	96 (88)
10	3.0 equiv of TMDS[c]	93 (85)
11	1.5 equiv of TMCTS[b]	99 (83)
12	4.0 equiv of PMHS	99 (96)
13	Ph-Bpin instead of PhB(OH)₂	49 (trace)

[a]Yields were determined through analysis by gas chromatography with the use of dodecane as an internal standard. [b]TMCTS = 2,4,6,8-tetramethylcyclotetrasiloxane. [c]TMDS = 1,1,3,3-tetramethyldisiloxane.

equiv of phenylsilane (PhSiH₃) as the terminal reductant with respect to limiting nitrobenzene (2) (Table 1, entry 1), but experiments show that fewer equivalents may be employed. Indeed, an excess of phenylsilane is not inherently required, and loadings as low as 0.77 equiv lead to qualitatively similar reaction outcomes (entry 6); lower loadings do, however, lead to diminished conversion and yield (entries 7 and 8). Taking into consideration that the reductive conversion of nitro-

benzene (2) to diphenylamine (4) is a two-fold reduction at N, the inference from these experiments is that all three Si−H reducing equivalents from phenylsilane can be leveraged for productive C−N coupling. With its low molecular weight and low effective mass per Si−H equivalent, phenylsilane could therefore be considered a rather efficient terminal reductant for the P^{III}/P^{V}=O-catalyzed C−N coupling reaction. We note, moreover, that hydrosilane equivalency shows no influence on reaction time (Table S2, entries 12−26), which has implications for its mechanistic role in mediating P^{III}/P^{V}=O catalysis (vide infra).

The reaction does not strictly require PhSiH₃ as the hydrosilane terminal reductant, but instead a wide range of common silicon-based reducing reagents are able to be interfaced with the P^{III}/P^{V}=O-catalyzed reductive C−N coupling. Along with Ph₂SiH₂ (Table 1, entry 9), a variety of siloxane-based reductants including 1,1,3,3-tetramethyldisiloxane (TMDS, Table 1, entry 10), 2,4,6,8-tetramethylcyclotetrasiloxane (TMCTS, Table 1, entry 11), and poly-(methylhydro)siloxane (PMHS, Table 1, entry 12) are viable.[18] Of these, PMHS is particularly attractive due to its ease of handling and low cost, recommending it for further method development.

As previously observed, the aryl C−N coupling reaction is most effective when arylboronic acid coupling partners are employed. Even under optimal reaction conditions, the use of phenylboronic acid pinacol ester (Ph−Bpin) in place of phenylboronic acid (3) results in only trace formation of coupling product 4 (Table 1, entry 13). The lower overall observed conversion (49%) is connected to substantial catalyst decomposition when the less-efficient boronate partner is employed.

2.1.4. Modified Conditions Enable Coupling of Previously Challenging Partners. With an eye toward an expanded scope for the P^{III}/P^{V}=O-catalyzed reductive C−N coupling method, we sought to determine if the versatility of the reaction conditions observed in the foregoing sections would provide an opportunity to approach previously problematic classes of coupling partners. The reaction of 1-methyl-5-nitroindole (5) with 4-fluorophenylboronic acid (6) is an illustrative example (Table 2). When applying typical first-generation reaction conditions (Table 2, entry 1), only 13% yield was obtained of the desired reductive coupling product 7. However, consistent with the solvent effect reported in section 2.1.1, a solvent

Table 2. Impact of Reaction Variables on Reductive C−N Coupling of Heterocyclic Nitroarenes
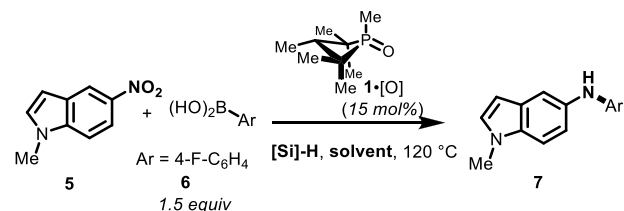
entry	SiH (equiv)	solvent	yield (%)[a]
1	PhSiH₃ (2)	m-xylene (0.25 M)	13
2	PhSiH₃ (2)	CPME (0.25 M)	27
3	PMHS (6)	m-xylene (0.25 M)	47
4	PMHS (6)	CPME (0.25 M)	68 (66)[b]

[a]Yields were determined through analysis by ¹⁹F NMR with the aid of 4-fluorotoluene as an internal standard. [b]Isolated yield in parentheses.

change to CPME resulted in a somewhat improved yield (27%, entry 2). Even more significantly, though, use of the hydrosilane reductant PMHS in *m*-xylene resulted in significantly improved yields (47%, Table 2, entry 3). The beneficial solvent and hydrosilane effects are synergistic in this case, such that the reaction of **5** and **6** conducted with PMHS in CPME provides coupling product **7** in a preparatively useful yield (68%, Table 2, entry 4).

These "second-generation" conditions (i.e., catalyst, 15 mol % 1,2,2,3,4,4-hexamethylphosphetane oxide (**1·[O]**); reductant, poly(methylhydro)siloxane; solvent, CPME) have been found to provide a general improvement in yield for all C−N coupling reactions we have assayed to date, and especially so for a variety of five- and six-membered heterocyclic nitroarenes that had previously been challenging to the intermolecular reductive P^{III}/P^{V}=O-catalyzed C−N coupling method (Table 3). In addition to indole **7**, a range of heteroarylnitro substrates are converted with reductive C−N coupling into the corresponding heteroarylamines as exemplified by pyrazole **8**, 2*H*-indazole **9**, pyrimidine **10**, and aminobenzothioazole **11**. Furthermore, reactions involving the incorporation of heteroaryl boronic acid coupling partners are similarly advantaged by the modified "second-generation" conditions; for instance, 1*H*-indazolyl (**12**), pyrazolyl (**13**), pyrimidinyl (**14**), and pyridinyl (**15**) boronic acids are successfully coupled with (hetero)aryl nitro partners. In all cases, though, the modified "second-generation conditions" afford marked improvements over the previously reported "first-generation conditions" and allow preparatively useful yields of functionally dense heteroarylamines. In instances where the heteroaryl boronic acid is found to be thermally unstable with respect to protodeboronation, a further modification to decrease the reaction temperature (80−100 °C) is found to be permissible (**12−14**).

2.2. Competition Studies: Intermolecular C−N Coupling vs Arylnitrene Reactivity. In an effort to delineate the relationship between the reductive C−N coupling reaction from previously reported P(III)/P(V)=O-catalyzed reactions of nitroarenes, we designed a set of competition experiments as described in Tables 4 and 5. As a point of reference, subjection of 2-nitrobiphenyl (**17**) to first-generation catalytic conditions with omission of the phenylboronic acid coupling partner resulted in formation of carbazole (**19**) by intramolecular cyclization (Table 4, entry 1).[15c] As previously reported, this C_{sp^2}−H amination reaction proceeds by two-fold sequential deoxygenation to give an arylnitrene that undergoes insertion to the proximal C−H position.[15c,19,58] We postulated that if similar arylnitrene intermediates were involved in the C−N cross coupling reaction with boronic acids, then a competition between intramolecular carbazole cyclization and intermolecular aryl amination with 2-nitrobiphenyl as a probe substrate would favor the former on kinetic grounds. In the event, reaction of 2-nitrobiphenyl (**17**) in the presence of phenylboronic acid **3** under otherwise identical reaction conditions led preferentially to the intermolecular reductive C−N cross coupling as the dominant reaction product (Table 4, entry 2). Notably, the use of CPME as the solvent (Table 4, entry 3) accentuates the bias in favor of the C−N cross coupling.

In a related fashion, intermolecular competition experiments are similarly inconsistent with formation of arylnitrenes on the pathway to C−N cross coupling. Deoxygenation of 4-nitrobenzonitrile (**20**) under conditions of P(III)/P(V)=O catalysis proves competent for arylnitrene generation, as inferred from *in situ* trapping with diethylamine to give azepine **22** as the major product (Table 5, entry 1).[20] However, when phenylboronic acid is admitted under otherwise identical reaction conditions, the reaction is shunted away from formation of azepine **22**, instead providing the diarylamine **21** by C−N coupling in good yield (Table 5, entry 2). As before, CPME as the solvent (Table 5, entry 3) further favors formation of the C−N cross coupling product **21** relative to azepine **22**.

The implications of these results are two-fold. First, the C−N cross coupling reaction evidently does not result from amination of the arylboronic acids by a free arylnitrene, but rather the mechanistic branching point along the pathway leading to cyclization or coupling must precede arylnitrene formation. Second, the impact of CPME on the product ratio suggests that the qualitative solvent effect observed in section 2.1.1 may arise through the relative suppression of the nitrene-forming pathway, which is nonproductive with respect to intermolecular C−N bond formation.

2.3. *In Situ* Spectroscopic Studies. *2.3.1. Catalyst Speciation in Reductive C−N Coupling.* In order to evaluate the catalyst speciation, *in situ* ^{31}P NMR spectra (161.9 MHz, 100 °C) were recorded under conditions of catalysis for the coupling reaction of nitrobenzene and phenylboronic acid (1.0

Table 3. Examples of Reductive C−N Coupling of Heterocyclic Nitroarenes and/or Boronic Acids[a]
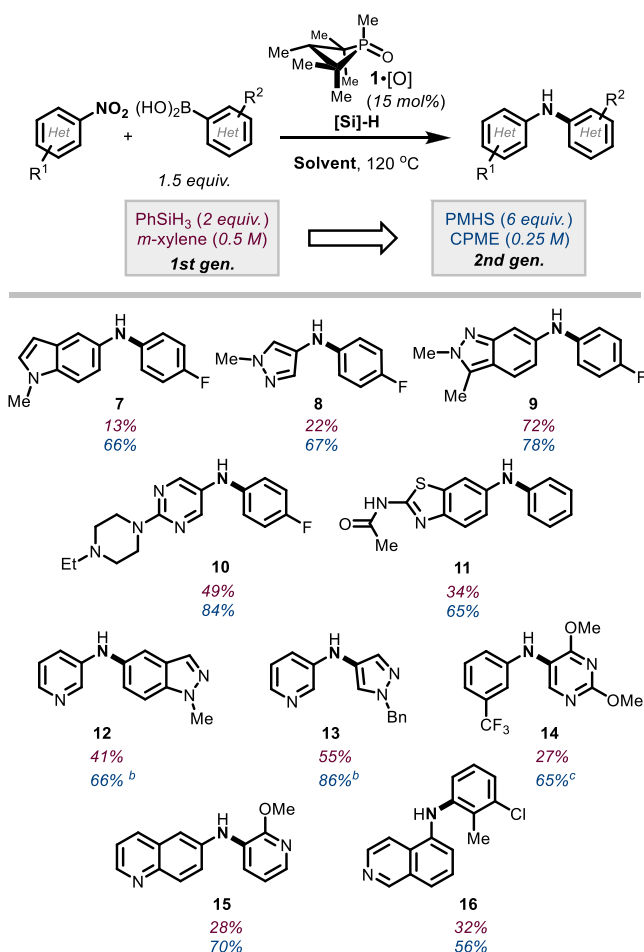
[a]Yields reported for isolated products. [b]Reaction was conducted at 100 °C. [c]Reaction was conducted at 80 °C. See Supporting Information for full experimental details.

Table 4. Competition Studies between Reductive C−N Coupling and Arylnitrene Reactivity Starting from 2-Nitrobiphenyl
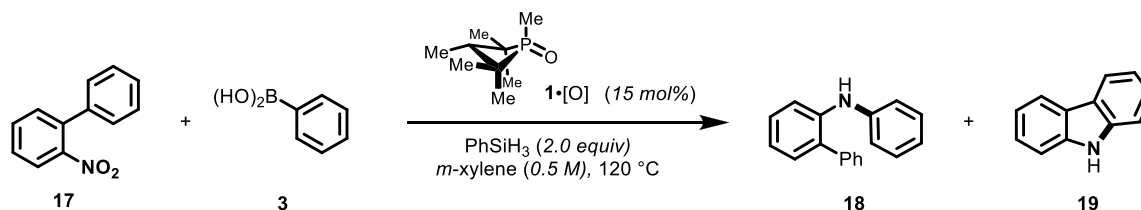
entry	equiv of boronic acid (3)	solvent	yield of 18 (%)[a]	yield of 19 (%)[a]
1	0	*m*-xylene	—	82
2	1.1	*m*-xylene	76	22
3	1.1	CPME	88	11

[a]Yields were determined through analysis by gas chromatography with the use of 1,3,5-trimethoxybenzene as an internal standard.

Table 5. Competition Studies between Reductive C−N Coupling vs Arylnitrene Reactivity Starting from 4-Nitrobenzonitrile
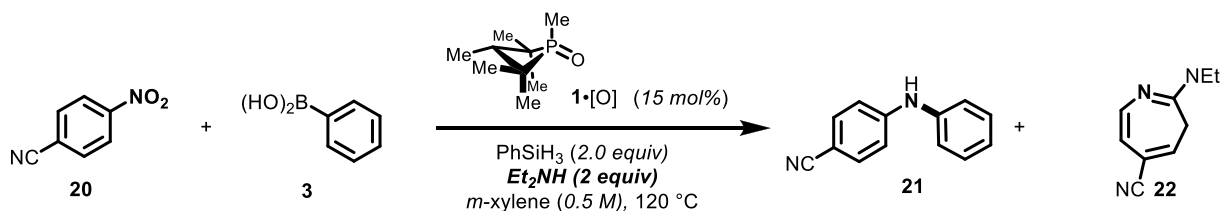
entry	equiv of boronic acid (3)	solvent	yield of 21 (%)[a]	yield of 22 (%)[a]
1	0	*m*-xylene	—	78
2	1.1	*m*-xylene	87	<2
3	1.1	CPME	93	<2

[a]Yields were determined through analysis by ^{1}H NMR spectroscopy with the aid of dibromomethane as an internal standard.

equiv of **2**, 1.1 equiv of **3**, 15 mol% of **1**·[O], 2 equiv of phenylsilane, 0.2 M in toluene-d_8. These spectra showed that phosphetane oxide **1**·[O] (δ 55.9 ppm) is rapidly converted ($t_{1/2} \approx 5$ min) to the corresponding tricoordinate phosphetane epimers *anti*-**1** and *syn*-**1** (δ 32.9 and δ 19.2 ppm, respectively)[21] (Figure 3). Over the ensuing reaction time

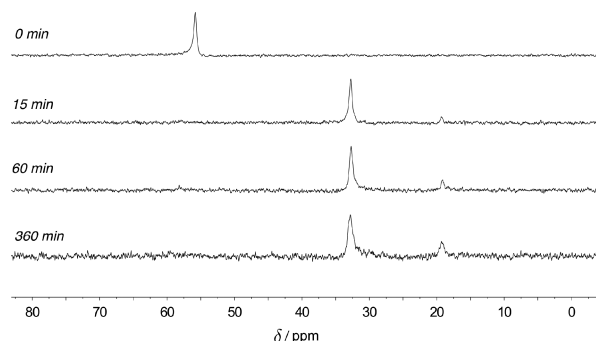**Figure 3.** Time-stacked *in situ* ^{31}P NMR spectra ($T = 100$ °C, toluene-d_8) at $t = 0$, 15, 60, and 360 min. Chemical shifts: **1**·[O], δ 55.9 ppm; **1**, δ 32.9 (*anti*) and 19.2 (*syn*) ppm. Units of chemical shift (δ) are ppm relative to 85% H_3PO_4 as an external standard.

during which **2** is converted to **4**, the tricoordinate epimers of **1** remain the only observable phosphorus-containing compounds in solution. Evidently, reduction of the phosphetane oxide **1**·[O] is quite swift and the reduced tricoordinate phosphetane **1** represents the resting state with respect to the catalytic phosphorus component. These observations run counter to prevailing notions about the kinetic inertness of phosphine oxides and provide evidence for the exceptional

reactivity of phosphetane oxide **1**·[O] as a biphilic O-atom transfer catalyst.

2.3.2. Reactant Speciation in Reductive C−N Coupling. ^{1}H NMR spectra (400 MHz, 100 °C) of a catalytic reaction show consumption of nitrobenzene over ca. 3 h with concomitant appearance of diphenylamine **4** as the major product (Figure 4). ^{15}N NMR spectra (40.5 MHz, 100 °C)
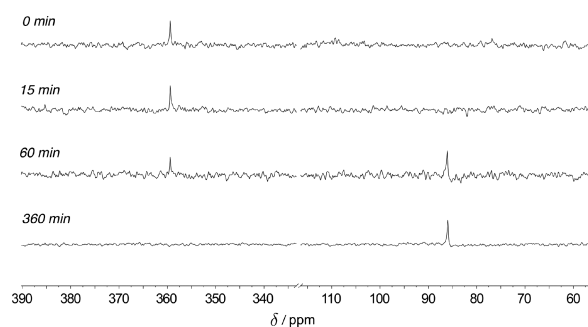

Figure 4. Time-stacked *in situ* ^{15}N NMR spectra ($T = 100$ °C, toluene-d_8) at $t = 0$, 15, 60, and 360 min. Chemical shifts: **2**, δ 369.4 ppm; **4**, δ 86.0 ppm. Units of chemical shift (δ) are ppm relative to $NH_{3(l)}$ as an external standard.

collected under identical conditions indicate that isotopically enriched ^{15}N-nitrobenzene (δ 369.4 ppm) is cleanly converted into the product diphenylamine (δ 86.0 ppm), and no long-lived intermediates are observed in the range 950 ppm > δ > −50 ppm (Figure S1).

2.4. Catalytic Kinetics Experiments. The kinetic progress of the catalytic coupling of nitrobenzene **2** and phenylboronic acid **3** was monitored via ex situ HPLC analysis

of reaction aliquots drawn at intervals over the course of 7 h. Nitrobenzene **2** is converted to diphenylamine **4** in >95% efficiency with no discernible intermediates (chromatograms in Figure S4), consistent with the observations from NMR spectroscopy. The decrease in concentration of starting material **2** as a function of time fits a first-order kinetic model (Figure 5A), where the initial rates vary linearly with
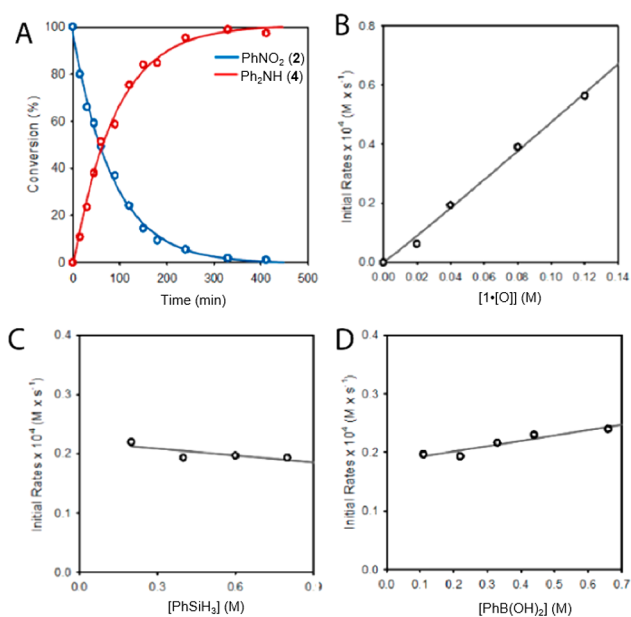

Figure 5. Spectroscopic and experimental mechanistic investigations. (A) Plot of conversion of substrate **2** (blue) to product **4** (red) vs time. (B) Plot of initial rates for substrate **2** consumption vs precatalyst **1**·[O] concentration. (C) Plot of initial rates for substrate **2** consumption vs phenylsilane concentration. (D) Plot of initial rates for substrate **2** consumption vs phenylboronic acid **3** concentration.

precatalyst **1**·[O] concentration in the range 0.02 M $\leq$ [**1**·[O]] $\leq$ 0.08 M (Figure 5B), indicating that the reaction in Figure 3 is first-order with respect to both substrate **2** and precatalyst **1**·[O]. Rate constants obtained by the complementary monitoring of increasing product **4** concentration with time at varying precatalyst **1**·[O] concentrations (Figure S6) agree within ±10%. Initial reaction rates measured for this catalytic reaction vary neither as a function of phenylsilane concentration (0.2 M < [PhSiH$_3$] < 0.8 M], Figure 5C) nor phenylboronic acid (**3**) concentration (0.1 M < [**3**] < 0.7 M], Figure 5D). The empirical rate law for the catalytic C−N coupling therefore is described by the equation:

$$\nu = k_{expt}[\mathbf{1}\cdot(\mathrm{O})]^1[\mathbf{2}]^1[\mathbf{3}]^0[\mathrm{PhSiH}_3]^0$$

2.5. Computational Studies. *2.5.1. Initial Deoxygenation and Rate-Determining Step.* Density functional theory calculations, conducted at the M06-2X/6-311++G(d,p) level with a polarizable continuum model (PCM) for solvation in *m*-xylene (ε = 2.3478), provide an atomistic-level proposal of mechanism that agrees with spectroscopic and kinetic studies. In accordance with our previous calculations on nitroarene−phosphine reactivity,[15c] DFT predicts a stepwise pathway for reductive C−N coupling initiated by a (3+1) cheletropic addition of nitrobenzene **2** with phosphetane **1** to form pentacoordinate spiro-bicyclic dioxazaphosphetane **Int-1** (Figure 6A). The transition state for the concerted (3+1) addition step can be viewed as a Woodward−Hoffmann allowed

$[_4\pi_s+_2\omega_s]$ cycloaddition (**TS-1**, Figure 6B) with a computed barrier of $\Delta G^{\ddagger}_{rel}$ = +31.0 kcal/mol). By virtue of this relatively high barrier, passage through **TS-1** represents the slowest step in the computed pathway, kinetically gating all downstream events and providing a rationale for the failure to spectroscopically detect any reaction intermediates. Dioxazaphosphetane **Int-1** evolves by a retro-(2+2) fragmentation with a low kinetic barrier via **TS-2** (Figure 6B, $\Delta G^{\ddagger}_{rel}$ = +10.8 kcal/mol) to give phosphine oxide **1**·[O] and nitrosobenzene (**Int-2**) (ΔG_{rel} = −31.9 kcal/mol). The lower activation barrier calculated for the collapse of the spirobicyclo **Int-1** (via **TS-2**) relative to its formation (via **TS-1**) stems from the incipient dissociation of *P*-oxide **1**·[O] and release of ring strain during the fragmentation.

EDA-NOCV calculations[22,23] of the charge flow and pairwise orbital interactions of **TS-1** validate the biphilic character of phosphetane **1**. Electrostatic (ΔE_{elstat} = −81.1 kcal/mol) and orbital interactions (ΔE_{orb} = −68.2 kcal/mol) between the phosphetane **1** and nitrobenzene **2** fragments are attractive and comparable in magnitude, accounting for 54.3% and 45.7% of the bonding interactions, respectively. Together, ΔE_{elstat} and ΔE_{orb} offset the Pauli electron pair repulsion term (ΔE_{Pauli} = 137.8 kcal/mol) to afford a total bonding energy of −11.5 kcal/mol. Analysis of the deformation densities displays both the electron donation from the HOMO of phosphetane **1** to the LUMO of nitrobenzene **2** and the backward electron donation from the HOMO of nitrobenzene **2** to the LUMO of phosphetane **1**. The main deformation density (Δq^{d}_{σ} = −1.0592) corresponds to a strong σ-donation from the phosphorus lone pair to the nitroarene and contributes to a stabilization of −56.8 kcal/mol (Figure 7A). An additional deformation densities with a smaller contribution (Δq^{bd}_{π} = −0.2823) is consistent with π-backdonation from the nitroarene to the P−C σ* antibonding orbitals of the phosphetane and provide a considerable stabilization of −9.0 kcal/mol (Figure 7B).

A second-order perturbation natural bond orbital (NBO)[24,25] analysis of **TS-1** affords additional insight into donor−acceptor interactions. Phosphorus lone pair σ-donation is represented by incipient σ P−O bonds polarized toward the oxygen that display an approximate composition of 38.52% P(sp$^{3.64}$) + 61.48% O(sp$^{23.53}$). Interestingly, endocyclic σ P−C bonds of the phosphetane, which are polarized toward the carbon and present an approximate composition of 37.41% P(sp$^{2.44}$) + 62.59% C(sp$^{4.40}$), also act as donors delocalized into the geminal acceptor σ* P−O bonds. In contrast, π-symmetry back-donation from the nitroarene moiety entails delocalization of both the σ P−O bonds and the O lone pairs into the geminal σ* P−C antibonding orbitals with relative second-order perturbation energies consistent with a 4:1 donor prevalence of the σ P−O bonds over the O lone pairs.

2.5.2. Second Deoxygenation and Product-Forming Step. Once formed, nitrosobenzene (**Int-2**) itself is subject to reaction with phosphetane **1** (Figure 7C) to give an oxazaphosphirane intermediate **Int-3** (ΔG_{rel} = −1.0 kcal/mol). Isomeric transition structures **TS-3a** and **TS-3b**, differing in the trajectory for the phosphetane attack on **Int-2**, were located. Both structures describe an asynchronous (2+1) addition with a P-centered spiro geometry that facilitates the interaction of the phosphorus lone pair with the π* orbital of the N=O group. **TS-3a**, which corresponds to the attack of the phosphorus on the nitrogen of the N=O group,[26] is favored by 8.1 kcal/mol relative to **TS-3b**, which represents the
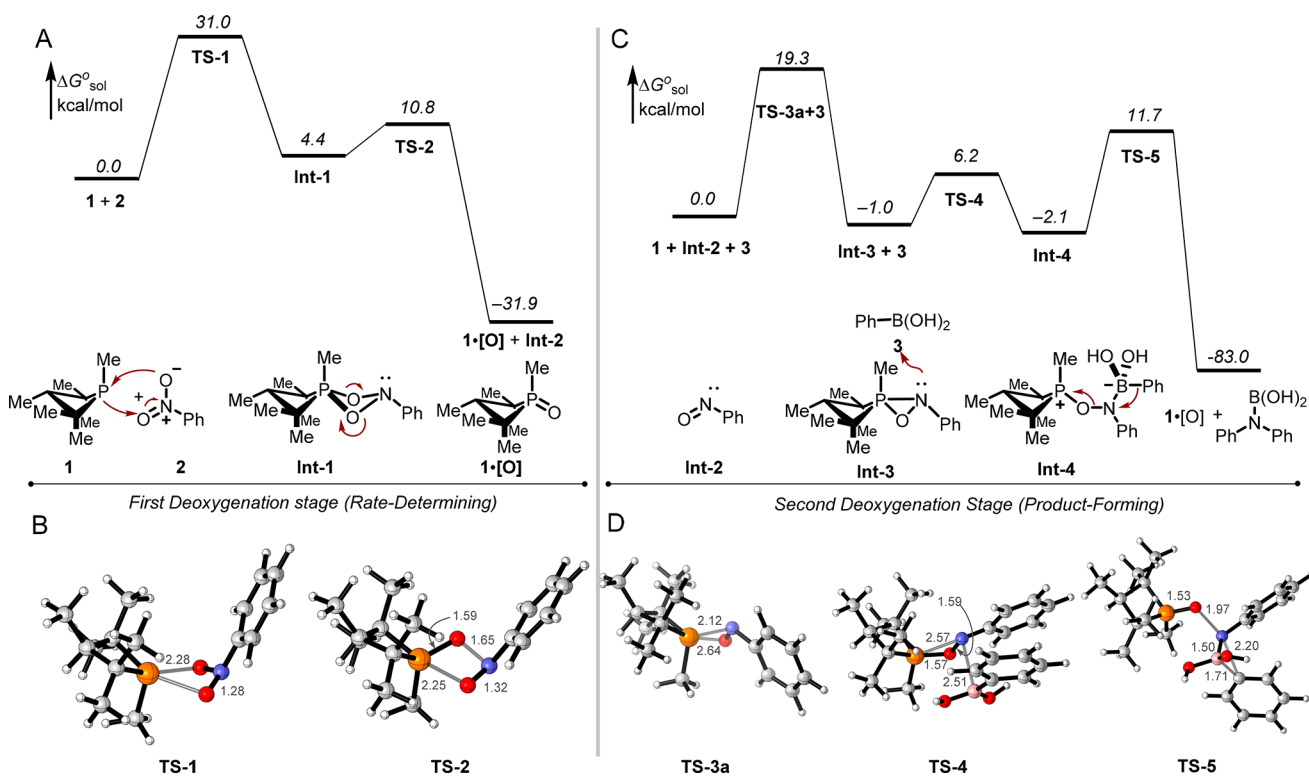
Figure 6. Mechanistic proposal for catalytic reductive C−N coupling supported by density functional theory (DFT) calculations at the M06-2X/6-311++G(d,p)/PCM(*m*-xylene) level of theory. Relative free energies (italics) are given in kcal/mol. (A) Proposed mechanism of initial nitrobenzene deoxygenation and rate-determining step. (B) Computed model of **TS-1** and **TS-2**. (C) Proposed mechanism of second deoxygenation and product-forming step. (D) Computed model of **TS-3a**, **TS-4**, and **TS-5**. Phosphorus (orange), oxygen (red), nitrogen (blue), carbon (gray), boron (pink), hydrogen (white). Bond distances in Å.
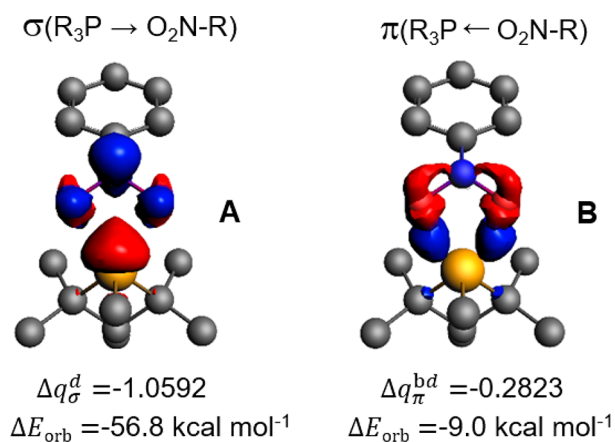

Figure 7. EDA-NOCV results of the orbital interactions for the (3+1) cheletropic addition of nitrobenzene **2** with phosphetane **1** to form pentacoordinate spiro-bicyclic dioxazaphosphetane **Int-1**. Red = depletion, blue = accumulation. (A) Forward electron donation. (B) Backward electron donation.

attack of the phosphorus on the oxygen[27] in agreement with a prevalence of the LUMO coefficient of the N═O group at the nitrogen atom.[28] Electrophilic ring opening of oxazaphosphirane **Int-3** with phenylboronic acid via **TS-4** ($\Delta G^{\ddagger}_{rel}$ = +6.2 kcal/mol) coincides with the favorable formation of phosphonium oxyaminoborate betaine **Int-4** (ΔG_{rel} = −2.1 kcal/mol), featuring a typical aminoboronate B−N bond length and an intramolecular charge-dipole contact between the phosphorus and the OH group of the aminoborate moiety. As a suitable zwitterionic retron for 1,2-metalate rearrange-

ment,[24,29] **Int-4** represents the immediate precursor to C−N bond formation, evolving via **TS-5** ($\Delta G^{\ddagger}_{rel}$ = +11.7 kcal/mol) with departure of phosphine oxide **1**·[O] by antiperiplanar migration of the phenyl group from boron to nitrogen to give phenylboramidic acid (Figure 7D).

A DFT analysis of the competition between the Cadogan cyclization and the reductive C−N coupling pathways for 2-nitrobiphenyl (**17**) qualitatively supports the experimental preference for C−N coupling discussed in section 2.2 (Tables 4 and 5).[30] Following a rate-limiting first deoxygenation of the nitro group by phosphetane **1** (**TS-6**, $\Delta G^{\ddagger}_{rel}$ = +29.7 kcal/mol) to afford 2-nitrosobiphenyl (**23**) (Figure 8A), reaction of the nitroso group with **1** takes place via a significantly lower barrier (**TS-8**, $\Delta G^{\ddagger}_{rel}$ = +17.2 kcal/mol) to give the "branching" intermediate oxazaphosphirane **Int-6**. In the Cadogan cyclization pathway, **Int-6** evolves through loss of phosphetane P-oxide **1**·[O] (**TS-9**, $\Delta G^{\ddagger}_{rel}$ = +15.0 kcal/mol) to form the carbazole product (**19**) via C−H insertion of the biphenylnitrene **Int-7** (**TS-10**, $\Delta G^{\ddagger}_{rel}$ = +8.9 kcal/mol).[15c] Alternatively, in the reductive C−N coupling pathway, **Int-6** reacts with phenylboronic acid (**TS-11**, $\Delta G^{\ddagger}_{rel}$ = +9.9 kcal/mol) to generate phosphonium oxyaminoborate betaine **Int-8**, which undergoes 1,2-metalate rearrangement and dissociation of phosphetane P-oxide **1**·[O] (**TS-12**, $\Delta G^{\ddagger}_{rel}$ = +12.2 kcal/mol). Inspection of the nonlimiting steps that intervene in the branching of oxazaphosphirane **Int-6** suggests that the experimental preference for reductive C−N coupling can be attributed to the circumvention of the biphenylnitrene pathways that mediates the Cadogan cyclization via a higher energy barrier **TS-9** (Figure 8B).
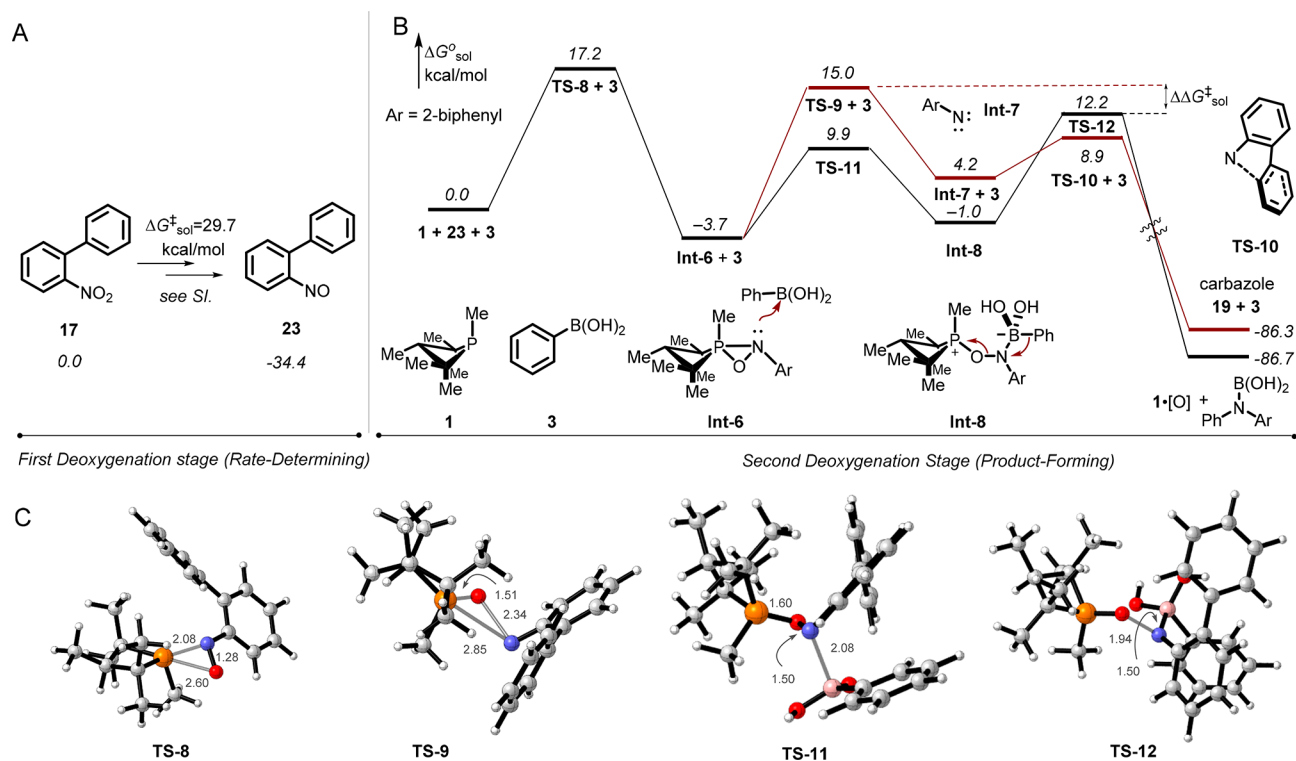
Figure 8. DFT studies (M06-2X/6-311++G(d,p)/PCM(*m*-xylene)) for the competition between intramolecular Cadogan cyclization and intermolecular reductive C−N coupling. (A) Initial deoxygenation with 2-nitrobiphenyl. (B) Proposed mechanism of second deoxygenation and product-forming step. (C) Computed models of **TS-8**, **TS-9**, **TS-11**, and **TS-12**. Phosphorus (orange), oxygen (red), nitrogen (blue), carbon (gray), boron (pink), hydrogen (white). Bond distances in Å.

3. DISCUSSION

As a complement to established net redox neutral (Buchwald−Hartwig and related) and net oxidative (Chan−Lam) transition-metal-catalyzed C−N coupling methods, the current method brings together nitroarene and arylboronic acid coupling partners through net reductive catalysis enabled by the P(III)/P(V)=O redox couple. Nitroarenes are attractive coupling partners because they are readily accessible and easily transformed in synthesis; the nitro functional group is both easily installed and strategically useful due to its powerful inductive effect.[31] And while nitroarenes are common precursors to aryl amine and aryl halide substrates for known transition-metal-catalyzed couplings, they are less commonly used as substrates themselves for direct catalytic C−N bond-forming reactions. Precedent within this vein includes the work of Nicholas, who established iron-catalyzed reductive C−N bond construction by reaction of nitroarenes with alkynes;[32] Baran, who has discovered an iron-catalyzed synthesis of N-alkylamines by reductive C−N bond formation between nitroarenes with alkenes;[33] and Shaver and Thomas, who have described related transformations catalyzed by an iron bis(phenolato)amine catalyst.[34] Hu has reported iron- and nickel-catalyzed reductive C−N bond formation by reaction of nitroarenes with alkyl and acyl electrophiles, respectively.[35] Apart from these catalytic methods, there exist several reagent-based approaches to direct conversion of nitroarenes to the corresponding N-functionalized anilines. Knochel[36] and Kürti[37] have demonstrated the use of excess Grignard reagents to convert nitroarenes to N-arylanilines directly. Niggemann has found that the combination of nitroarenes with organozinc reagents in the presence of stoichiometric B$_2$pin$_2$ results in

reductive conversion to N-functionalized anilines.[38] Recent works from our group[39] and Csáký[40] have validated a stoichiometric, phosphine-mediated reductive coupling of nitroarenes and arylboronic acids. Relatedly, Suárez-Pantiga and Sanz reported that phosphine-mediated reductive coupling of nitroarenes and boronic acids is catalyzed by an oxomolybdenum compound.[41] Among these varied approaches, the P(III)/P(V)=O-catalyzed method—with its relatively mild conditions, commercial catalyst, and inexpensive reductant—compares rather favorably.

With regard to the mechanism of the P(III)/P(V)=O-catalyzed reductive C−N coupling reaction, the combined experimental and computational data point toward a catalytic reaction sequence that evolves in two stages—an initial deoxygenation of the nitroarene substrate to the corresponding nitrosoarene (Figure 9, top hemisphere), and a subsequent second deoxygenation that converts the intermediate nitrosoarene into the observed N-arylated product (Figure 9, bottom hemisphere). The common thread uniting these two sequential reduction events is the action of the small-ring phosphacycle **1**·[O] to catalyze O-atom transfer by redox cycling in the P(III)/P(V) couple. Since O'Brien's initial report of an organophosphorus-catalyzed Wittig reaction,[42,43] P(III)/P(V) redox catalysis has emerged as an productive area of organophosphorus catalysis,[44−46] with work from Woerpel,[47] Rutjes and van Delft,[48] Werner,[49] Mecinović,[48g] Kwon,[50] and Voituriez[51] among others.[52−55] In the context of the current C−N coupling method, the observation that the resting state of the catalyst resides at the P(III) oxidation state (i.e., phosphetane **1**) confirms the swift deoxygenation kinetics of small-ring phosphine oxides noted by Marsi[56] and Keglevich[57] and makes clear that P(V)=O→P(III) turnover
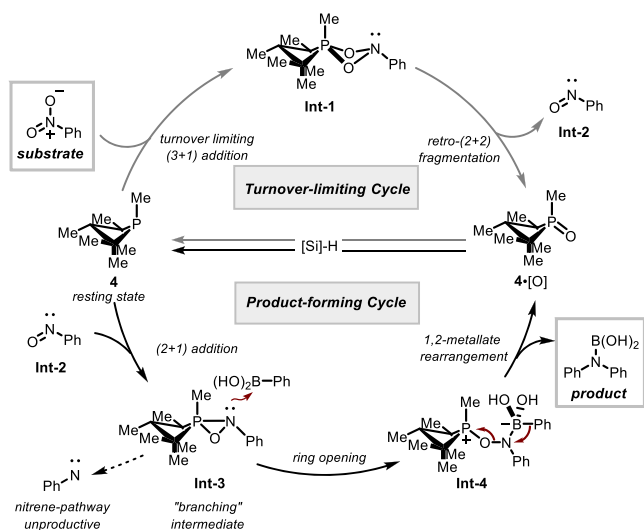
Figure 9. Proposed mechanism for organophosphorus-catalyzed reductive C−N coupling.

is not a significant impediment to method development in the P(III)/P(V) couple with these catalytic structures.

The initial nitroarene-to-nitrosoarene deoxygenation event is gated by a (3+1) cheletropic addition of nitrobenzene **2** with phosphetane **1**. Consistent with experimental spectroscopy and kinetics, DFT modeling confirms that this step is turnover limiting and highest in energy of any transition state in the entire reductive C−N coupling sequence. Analysis of the transition structure within both the EDA-NOCV and NBO theoretical frameworks validates the notion of pairwise orbital interactions allowing for *electron flow both to and from the phosphorus site*, in accord with the concept of "biphilic" (i.e., synergistic single-site donor/acceptor) reactivity of the phosphetane. The relative magnitudes of the donor and acceptor interactions suggest that the former predominates, which is consistent with Hammett studies (see SI) indicating a net transfer of electron density to the nitroarene in the transition state.[58,59] Once formed, **Int-1** evolves via retro-(2+2) fragmentation to liberate phosphetane oxide **1·[O]** and nitrosobenzene (**Int-2**), an obligate albeit unobserved intermediate under catalytic conditions. The phosphetane oxide **1·[O]** is itself subject to rapid deoxygenation by hydrosilane to return to the P(III) resting state (**1**) and close the first catalytic deoxygenation cycle.

The second deoxygenation stage commences with capture of nitrosobenzene (**Int-2**) by P(III) phosphetane **1** through an asynchronous (2+1) addition to provide an oxazaphosphirane **Int-3**. On the basis of product distributions obtained from competition studies between intermolecular C−N coupling vs arylnitrene reactivity, we posit that this oxazaphosphirane **Int-3** serves as the pivotal "branching" intermediate whose fate is a key determinant of product distribution. Whereas unimolecular loss of phosphetane oxide **1·[O]** from **Int-3** liberates an arylnitrene reactive intermediate that results in azepine ring expansion or Cadogan cyclization (cf. **TS-9**), DFT predicts a low-energy bimolecular reaction of oxazaphosphirane **Int 3** with arylboronic acid leads to heterolytic ring-opening (cf. **TS-4**) and formation of betaine **Int-4**. We surmise that the apparent solvent influence in the competition experiments (section 2.1) operates by stabilization of partial charge build-up in the transition states leading to and from dipolar structure

Int-4 (i.e., **TS-4** and **TS-5**), relative to dissociative loss of phosphetane oxide **1·[O]**. In analogy to numerous related electrophilic amination reactions of organoboron reagents,[24,38a,60−63] an ensuing 1,2-metalate rearrangement of betaine **Int-4** results in the formation of the desired C−N bond, which either upon hydrolysis with adventitious water or upon workup gives the target amine. A final hydrosilane-mediated reduction of phosphetane oxide **1·[O]** returns the catalyst to the P(III) resting state (**1**) and closes the second catalytic deoxygenation cycle.

4. CONCLUSION

P(III)/P(V)═O-catalyzed intermolecular reductive C−N cross coupling of nitroarenes and arylboronic acids is emerging as an operationally robust and mechanistically well-defined main-group complement to the established transition-metal-based methods for catalytic intermolecular C−N coupling. Combined experimental, spectroscopic, and computational experiments provide a description of the biphilic organophosphorus-catalyzed method by systematically differentiating the nature of deoxygenative events of nitroaromatics especially in the context of the C−N bond formation. Namely, the rate-determining step is a (3+1) addition. The product-determining step involves the ring-opening of an oxazaphosphirane. Combined, these findings enrich the fundamental understanding of the biphilic reactivity of phosphetanes as generalized platforms for catalytic reductive O-atom transfer operating in the P^{III}/P^V═O redox manifold and provide an experimentally based mechanistic framework to guide iterative catalyst design and method development.

5. EXPERIMENTAL SECTION

A full description of the general experimental methods can be found in the Supporting Information.

5.1. Representative Synthetic Procedure for the Reductive C−N Coupling. The appropriate nitro substrate (if solid) and phosphetane oxide precatalyst **1·[O]** (15 mol% unless otherwise noted) were added to an oven-dried glass culture tubes with threaded end (20 × 125 mm; Fisher Scientific part no. 14-959-35A), outfitted with a phenolic screw-thread open top cap (Kimble-Chase part no. 73804-15425) and PTFE-lined silicone septum (Thermo Fisher part no. B7995-15) sequentially. Following evacuation and the introduction of nitrogen on a Schlenk line, dry CPME was added via syringe. Lastly, hydrosilane and nitro substrate (if liquid) were added and the reaction mixture was stirred at 120 °C. When complete, the reaction vessel screw cap was unscrewed (note that in some cases pressure release was observed) and 10 mL of distilled water was added. With the aid of ethyl acetate, the reaction mixture was transferred to a separatory funnel. After mixing and separation of the aqueous layer, the organic layer was washed with 10 mL of a 1 M NaOH aqueous solution and 10 mL of brine. Each aqueous phase was back-extracted with 10 mL portions of ethyl acetate. The combined organic layers were dried over anhydrous sodium sulfate, filtered, and concentrated with the aid of a rotary evaporator. The crude residues were purified via column chromatography to yield pure coupling products. Columns were primarily slurry packed with hexanes, and mobile-phase polarity was increased gradually to the mixture indicated.

5.2. Spectroscopic Investigations. To an oven-dried purged septum-sealed NMR tube were added ^{15}N-labeled nitrobenzene (12 mg, 0.10 mmol, 1.0 equiv), phenylboronic acid **3** (11 mg, 0.11 mmol, 1.1 equiv), and **1·[O]** (2.6 mg, 0.015 mmol, 15 mol%) in toluene-d_8 (0.5 mL). The tube was inserted into the NMR probe thermostated at 100 °C, and a $t = 0$ spectrum was obtained. The tube was ejected from the probe, phenylsilane (25 μL, 0.20 mmol, 2.0 equiv) was added via syringe, and the NMR tube was reinjected into the probe. [15]N (ppm is relative to $NH_{3(l)}$ external standard) and ^{31}P NMR

spectra (ppm is relative to 85% H_3PO_4 external standard) were collected at 15, 60, 180, and 360 min.

5.3. Kinetics Experiments. For a kinetic run corresponding to a single rate constant, a solution of nitrobenzene (**2**) and phosphetane P-oxide **1**·[O] in *m*-xylene was prepared under nitrogen in an oven-dried, three-neck round-bottom flask fitted with a silicon-tipped IR probe and a magnetic stir bar. The solution temperature was stabilized at 108 ± 2 °C, and the reaction was initiated by adding $PhSiH_3$. Reaction monitoring started 15 min after the addition of $PhSiH_3$ to ensure full reduction of **1**·[O], as determined by the disappearance of the *P*-oxide IR absorbance at 1199 cm^{-1}. Sample aliquots (20 μL ± 10%) were periodically taken using a calibrated automated sampler,[64] diluted at room temperature into acetonitrile (80×), and analyzed using an HPLC system equipped with a C18 column (4.6 × 50 mm) and an SPD-20A/20AV UV−vis detector. Good pseudo-first-order plots were obtained by monitoring the decay of nitrobenzene (**2**) and growth of diphenylamine (**4**) relative to a standard calibration curve, and the initial rates ($\Delta[2]/\Delta t$) were calculated by multiplying the pseudo-first-order reaction rate constants (exponential slopes) by the corresponding concentrations of nitrobenzene (**2**). Rates were shown to be reproducible within experimental error (±10%).

5.4. Computational Methods. Geometries were optimized in Gaussian 09[65] using the M06-2X[66] density functional with the 6-311++G(d,p) basis set. The calculated energies (ΔG, 298.15 K, 1.0 atm) result from the sum of electronic and thermal free energies as obtained from the frequency analysis at the same level of theory. Open-shell singlet energies were spin-projected.[67] Frequency calculations for all stationary points were carried out to describe them either as minima ($i = 0$) or as first-order transition states ($i = 1$). For all transition structures, visualization of the imaginary frequencies corresponded to the expected normal mode for the elementary step under investigation. Intrinsic reaction coordinate calculations were performed from the transition states in forward and reverse directions to confirm the lowest energy reaction pathways that connect the corresponding minima. See Supporting Information for further details.

ASSOCIATED CONTENT

ⓈⅠ Supporting Information

The Supporting Information is available free of charge at https://pubs.acs.org/doi/10.1021/jacs.0c01666.

> General methods, additional optimization, synthetic procedures; ^{1}H, ^{13}C, ^{15}N, and ^{31}P NMR spectra; kinetics data; spectroscopy data; computational details; and Cartesian coordinates, including Figures S1−S12 and Tables S1−S8 (PDF)

AUTHOR INFORMATION

Corresponding Author

Alexander T. Radosevich − *Department of Chemistry, Massachusetts Institute of Technology, Cambridge, Massachusetts 02139, United States;* ⓞ orcid.org/0000-0002-5373-7343; Email: radosevich@mit.edu

Authors

Gen Li − *Department of Chemistry, Massachusetts Institute of Technology, Cambridge, Massachusetts 02139, United States;* ⓞ orcid.org/0000-0001-6857-0235

Trevor V. Nykaza − *Department of Chemistry, Massachusetts Institute of Technology, Cambridge, Massachusetts 02139, United States;* ⓞ orcid.org/0000-0002-7683-2984

Julian C. Cooper − *Department of Chemistry, Massachusetts Institute of Technology, Cambridge, Massachusetts 02139, United States;* ⓞ orcid.org/0000-0001-8231-2654

Antonio Ramirez − *Chemical and Synthetic Development, Bristol-Myers Squibb Company, New Brunswick, New Jersey 08903, United States;* ⓞ orcid.org/0000-0003-2636-6855

Michael R. Luzung − *Chemical and Synthetic Development, Bristol-Myers Squibb Company, New Brunswick, New Jersey 08903, United States;* ⓞ orcid.org/0000-0001-9729-2211

Complete contact information is available at:
https://pubs.acs.org/10.1021/jacs.0c01666

Notes

The authors declare no competing financial interest.

■ ACKNOWLEDGMENTS

■ REFERENCES

(1) (a) Vitaku, E.; Smith, D. T.; Njardarson, J. T. Analysis of the structural diversity, substitution patterns, and frequency of nitrogen heterocycles among U.S. FDA approved pharmaceuticals. *J. Med. Chem.* **2014**, *57*, 10257. (b) Knölker, H.-J., Ed. *The Alkaloids: Chemistry and Biology*; Elsevier: San Diego, 2011; Vol. 70. (c) Ćiric-Marjanovic, G. Recent advances in polyaniline research: polymerization mechanisms, structural aspects, properties and applications. *Synth. Met.* **2013**, *177*, 1.

(2) (a) Hartwig, J. F. Carbon-Heteroatom Bond Formation Catalysed by Organometallic Complexes. *Nature* **2008**, *455*, 314. (b) Bariwal, J.; Van der Eycken, E. C−N Bond Forming Cross-coupling Reactions: an overview. *Chem. Soc. Rev.* **2013**, *42*, 9283.

(3) (a) Jiang, L.; Buchwald, S. L. Palladium-Catalyzed Aromatic Carbon-Nitrogen Bond Formation. In *Metal-Catalyzed Cross-Coupling Reactions*, 2nd ed.; De Meijere, A., Diderich, F., Eds.; Wiley-Blackwell: Hoboken, NJ, 2008; pp 699−760. (b) Dorel, R.; Grugel, C. P.; Haydl, A. M. The Buchwald−Hartwig Amination After 25 Years. *Angew. Chem., Int. Ed.* **2019**, *58*, 17118.

(4) For Ni-catalyzed reactions, see: (a) Marín, M.; Rama, R. J.; Nicasio, M. C. Ni-Catalyzed Amination Reactions: An Overview. *Chem. Rec.* **2016**, *16*, 1819. (b) Corcoran, E. B.; Pirnot, M. T.; Lin, S.; Dreher, S. D.; DiRocco, D. A.; Davies, I. W.; Buchwald, S. L.; MacMillan, D. W. C. Aryl Amination using Ligand-free Ni(II) Salts and Photoredox Catalysis. *Science* **2016**, *353*, 279. (c) Oderinde, M. S.; Jones, N. H.; Juneau, A.; Frenette, M.; Aquila, B.; Tentarelli, S.; Robbins, D. W.; Johannes, J. W. Highly Chemoselective Iridium Photoredox and Nickel Catalysis for the Cross-Coupling of Primary Aryl Amines with Aryl Halides. *Angew. Chem., Int. Ed.* **2016**, *55*, 13219. (d) Lim, C. H.; Kudisch, M.; Liu, B.; Miyake, G. M. C-N Cross-Coupling via Photoexcitation of Nickel-Amine Complexes. *J. Am. Chem. Soc.* **2018**, *140*, 7667.

(5) For Cu-catalyzed reactions, see: (a) Beletskaya, I. P.; Cheprakov, A. V. The Complementary Competitors: Palladium and Copper in C−N Cross-Coupling Reactions. *Organometallics* **2012**, *31*, 7753. (b) Sambiagio, C.; Marsden, S. P.; Blacker, A. J.; McGowan, P. C. Copper Catalysed Ullmann Type Chemistry: From Mechanistic Aspects to Modern Development. *Chem. Soc. Rev.* **2014**, *43*, 3525. (c) Bhunia, S.; Pawar, G. G.; Kumar, S. V.; Jiang, Y.; Ma, D. Selected Copper-Based Reactions for C-N, C-O, C-S, and C-C Bond Formation. *Angew. Chem., Int. Ed.* **2017**, *56*, 16136.

(6) (a) Hartwig, J. F. Transition Metal Catalyzed Synthesis of Arylamines and Aryl Ethers from Aryl Halides and Triflates: Scope and Mechanism. *Angew. Chem., Int. Ed.* **1998**, *37*, 2046. (b) Brusoe, A. T.; Hartwig, J. F. Palladium-Catalyzed Arylation of Fluoroalkylamines. *J. Am. Chem. Soc.* **2015**, *137*, 8460. (c) Peacock, D. M.; Roos, C. B.; Hartwig, J. F. Palladium-Catalyzed Cross Coupling of Secondary and Tertiary Alkyl Bromides with a Nitrogen Nucleophile. *ACS Cent. Sci.* **2016**, *2*, 647. (d) Peacock, D. M.; Jiang, Q.; Hanley, P. S.; Cundari, T. R.; Hartwig, J. F. Reductive Elimination from Phosphine-Ligated Alkylpalladium(II) Amido Complexes to Form Sp3 Carbon-Nitrogen Bonds. *J. Am. Chem. Soc.* **2018**, *140*, 4893.

(7) (a) Dennis, J. M.; White, N. A.; Liu, R. Y.; Buchwald, S. L. Breaking the Base Barrier: An Electron-Deficient Palladium Catalyst

Enables the Use of a Common Soluble Base in C-N Coupling. *J. Am. Chem. Soc.* **2018**, *140*, 4721. (b) Dennis, J. M.; White, N. A.; Liu, R. Y.; Buchwald, S. L. Pd-Catalyzed C-N Coupling Reactions Facilitated by Organic Bases: Mechanistic Investigation Leads to Enhanced Reactivity in the Arylation of Weakly Binding Amines. *ACS Catal.* **2019**, *9*, 3822.

(8) (a) Park, N. H.; Vinogradova, E. V.; Surry, D. S.; Buchwald, S. L. Design of New Ligands for the Palladium-Catalyzed Arylation of α-Branched Secondary Amines. *Angew. Chem., Int. Ed.* **2015**, *54*, 8259. (b) Ruiz-Castillo, P.; Blackmond, D. G.; Buchwald, S. L. Rational Ligand Design for the Arylation of Hindered Primary Amines Guided by Reaction Progress Kinetic Analysis. *J. Am. Chem. Soc.* **2015**, *137*, 3085. (c) Olsen, E. P. K.; Arrechea, P. L.; Buchwald, S. L. Mechanistic Insight Leads to a Ligand Which Facilitates the Palladium-Catalyzed Formation of 2-(Hetero)Arylaminooxazoles and 4-(Hetero)-Arylaminothiazoles. *Angew. Chem., Int. Ed.* **2017**, *56*, 10569.

(9) (a) Ingoglia, B. T.; Buchwald, S. L. Oxidative Addition Complexes as Precatalysts for Cross-Coupling Reactions Requiring Extremely Bulky Biarylphosphine Ligands. *Org. Lett.* **2017**, *19*, 2853. (b) Uehling, M. R.; King, R. P.; Krska, S. W.; Cernak, T.; Buchwald, S. L. Pharmaceutical diversification via palladium oxidative addition complexes. *Science* **2019**, *363*, 405.

(10) Ruiz-Castillo, P.; Buchwald, S. L. Applications of Palladium-Catalyzed C-N Cross-Coupling Reactions. *Chem. Rev.* **2016**, *116*, 12564.

(11) (a) Hall, D. G.; Wiley-VCH: Weinheim, 2005. (b) Fyfe, J. W. B.; Watson, A. J. B. Recent Developments in Organoboron Chemistry: Old Dogs, New Tricks. *Chem.* **2017**, *3*, 31.

(12) (a) King, A. E.; Brunold, T. C.; Stahl, S. S. Mechanistic Study of Copper-Catalyzed Aerobic Oxidative Coupling of Arylboronic Esters and Methanol: Insights into an Organometallic Oxidase Reaction. *J. Am. Chem. Soc.* **2009**, *131*, 5044. (b) King, A. E.; Ryland, B. L.; Brunold, T. C.; Stahl, S. S. Kinetic and Spectroscopic Studies of Aerobic Copper(II)-Catalyzed Methoxylation of Arylboronic Esters and Insights into Aryl Transmetalation to Copper(II). *Organometallics* **2012**, *31*, 7948. (c) Vantourout, J. C.; Law, R. P.; Isidro-Llobet, A.; Atkinson, S. J.; Watson, A. J. B. Chan-Evans-Lam Amination of Boronic Acid Pinacol (BPin) Esters: Overcoming the Aryl Amine Problem. *J. Org. Chem.* **2016**, *81*, 3942. (d) Vantourout, J. C.; Miras, H. N.; Isidro-Llobet, A.; Sproules, S.; Watson, A. J. B. Spectroscopic Studies of the Chan–Lam Amination: A Mechanism-Inspired Solution to Boronic Ester Reactivity. *J. Am. Chem. Soc.* **2017**, *139*, 4769.

(13) West, M. J.; Fyfe, J. W. B.; Vantourout, J. C.; Watson, A. J. B. Mechanistic Development and Recent Applications of the Chan–Lam Amination. *Chem. Rev.* **2019**, *119*, 12491.

(14) Kirby, A. J.; Warren, S. G. *The Organic Chemistry of Phosphorus*; Elsevier: Amsterdam, 1967; p 20.

(15) (a) Zhao, W.; Yan, P. K.; Radosevich, A. T. A Phosphetane Catalyzes Deoxygenative Condensation of α-Keto Esters and Carboxylic Acids via $P^{III}/P^V{=}O$ Redox Cycling. *J. Am. Chem. Soc.* **2015**, *137*, 616. (b) Nykaza, T. V.; Harrison, T. S.; Ghosh, A.; Putnik, R. A.; Radosevich, A. T. A Biphilic Phosphetane Catalyzes N–N Bond-Forming Cadogan Heterocyclization via $P^{III}/P^V{=}O$ Redox Cycling. *J. Am. Chem. Soc.* **2017**, *139*, 6839. (c) Nykaza, T. V.; Ramirez, A.; Harrison, T. S.; Luzung, M. R.; Radosevich, A. T. Biphilic Organophosphorus-Catalyzed Intramolecular Csp^2–H Amination: Evidence for a Nitrenoid in Catalytic Cadogan Cyclizations. *J. Am. Chem. Soc.* **2018**, *140*, 3103. (d) Nykaza, A. T. V; Li, G.; Yang, J.; Luzung, M. R.; Radosevich, A. T. *Angew. Chem., Int. Ed.* **2020**, *59*, 4505. (e) Ghosh, A.; Lecomte, M.; Kim-Lee, S.-H.; Radosevich, A. T. Organophosphorus-Catalyzed Deoxygenation of Sulfonyl Chlorides: Electrophilic (Fluoroalkyl)Sulfenylation by $P^{III}/P^V{=}O$ Redox Cycling. *Angew. Chem., Int. Ed.* **2019**, *58*, 2864. (f) Lecomte, M.; Lipshultz, J. M.; Kim-Lee, S.-H.; Li, G.; Radosevich, A. T. Driving Recursive Dehydration by P^{III}/P^V Catalysis: Annulation of Amines and Carboxylic Acids by Sequential C−N and C−C Bond Formation. *J. Am. Chem. Soc.* **2019**, *141*, 12507.

(16) Nykaza, T. V.; Cooper, J. C.; Li, G.; Mahieu, N.; Ramirez, A.; Luzung, M. R.; Radosevich, A. T. Intermolecular Reductive C-N Cross Coupling of Nitroarenes and Boronic Acids by $P^{III}/P^V{=}O$ Catalysis. *J. Am. Chem. Soc.* **2018**, *140*, 15200.

(17) Watanabe, K.; Yamagiwa, N.; Torisawa, Y. Cyclopentyl Methyl Ether as a New and Alternative Process Solvent. *Org. Process Res. Dev.* **2007**, *11*, 251.

(18) The number of total hydride equivalents was maintained when comparing different silane reagents.

(19) Tsao, M. L.; Gritsan, N.; James, T. R.; Platz, M. S.; Hrovat, D. A.; Borden, W. T. Study of the Chemistry of Ortho- and Para-Biphenylnitrenes by Laser Flash Photolysis and Time-Resolved IR Experiments and by B3LYP and CASPT2 Calculations. *J. Am. Chem. Soc.* **2003**, *125*, 9343.

(20) (a) Poe, R.; Schnapp, K.; Young, M. J. T.; Grayzar, J.; Platz, M. S. Chemistry and Kinetics of Singlet (Pentafluorophenyl)Nitrene. *J. Am. Chem. Soc.* **1992**, *114*, 5054. (b) Karney, W. L.; Borden, W. T. Ab Initio Study of the Ring Expansion of Phenylnitrene and Comparison with the Ring Expansion of Phenylcarbene. *J. Am. Chem. Soc.* **1997**, *119*, 1378. (c) Gritsan, N. P.; Likhotvorik, I.; Tsao, M. L.; Çelebi, N.; Platz, M. S.; Karney, W. L.; Kemnitz, C. R.; Borden, W. T. Ring-Expansion Reaction of Cyano-Substituted Singlet Phenyl Nitrenes: Theoretical Predictions and Kinetic Results from Laser Flash Photolysis and Chemical Trapping Experiments. *J. Am. Chem. Soc.* **2001**, *123*, 1425.

(21) The ^{31}P NMR chemical shifts of **1** and **1**·[O] exhibit temperature-dependent behavior. See the Supporting Information of ref 15b for plots of ^{31}P NMR chemical shift temperature dependence for *syn*-**1** and *anti*-**1**. The temperature dependence of ^{31}P NMR chemical shifts has been noted previously: Gordon, M. D.; Quin, L. D. Temperature Dependence of ^{31}P NMR Chemical Shifts of Some Trivalent Phosphorus Compounds. *J. Magn. Reson.* **1976**, *22*, 149.

(22) (a) The EDA-NOCV method, which combines energy decomposition analysis (EDA) with the natural orbital for chemical valence approach (NOCV), was executed as part of the Amsterdam Density Functional software package. (b) *ADF2014*, SCM; Theoretical Chemistry, Vrije Universiteit: Amsterdam, The Netherlands, http://www.scm.com (See Supporting Information for complete reference).

(23) (a) Mitoraj, M.; Michalak, A.; Ziegler, T. A Combined Charge and Energy Decomposition Scheme for Bond Analysis. *J. Chem. Theory Comput.* **2009**, *5*, 962. (b) Mitoraj, M.; Michalak, A.; Ziegler, T. On the Nature of the Agostic Bond between Metal Centers and β-Hydrogen Atoms in Alkyl Complexes. An Analysis Based on the Extended Transition State Method and the Natural Orbitals for Chemical Valence Scheme (ETS-NOCV). *Organometallics* **2009**, *28*, 3727.

(24) (a) Brown, H. C.; Kramer, G W.; Levy, A. B.; Midland, M. M. *Organic Syntheses via Boranes*; Wiley-Interscience, New York, 1975. (b) Brown, H. C.; Salunkhe, A. M.; Argade, A. B. Organoboranes. 55. Improved Procedure for the Conversion of Representative Achiral and Chiral Alkyl-, (E)-1-Alkenyl and (Z)-1-Alkenyl-, and Arylboronates into the Corresponding Organyldichloroboranes. *Organometallics* **1992**, *11*, 3094. (c) Phanstiel, O., IV; Wang, W. X.; Powell, D. H.; Ospina, M. P.; Leeson, J B. A. Synthesis of Secondary Amines via N-(Benzoyloxy)amines and Organoboranes. *J. Org. Chem.* **1999**, *64*, 803. (d) Matteson, D. S.; Kim, G. Y. Asymmetric Alkyldifluoroboranes and Their Use in Secondary Amine Synthesis. *Org. Lett.* **2002**, *4*, 2153. (e) Bagutski, V.; Elford, T. G.; Aggarwal, V. K. Synthesis of Highly Enantioenriched C-Tertiary Amines from Boronic Esters: Application to the Synthesis of Igmesine. *Angew. Chem., Int. Ed.* **2011**, *50*, 1080.

(25) Weinhold, F. In *Encyclopedia of Computational Chemistry*; Schleyer, P. v. R., Allinger, N. L., Clark, T., Gasteiger, J., Kollman, P. A., Schaefer, H. F., III, Schreiner, P. R., Eds.; John Wiley & Sons: Chichester, UK, 1998; Vol. 3, pp 1792−1811.

(26) Zhu, J. S.; Li, C. J.; Tsui, K. Y.; Kraemer, N.; Son, J.-H.; Haddadin, M. J.; Tantillo, D. J.; Kurth, M. J. Accessing Multiple Classes of 2H-Indazoles: Mechanistic Implications for the Cadogan and Davis-Beirut Reactions. *J. Am. Chem. Soc.* **2019**, *141*, 6247.

(27) Khursan, V. S.; Shamukaev, V. A.; Chainikova, E. M.; Khursan, S. L.; Safiullin, R. L. Kinetics and Mechanism of the Nitrosobenzene Deoxygenation by Trivalent Phosphorous Compounds. *Russ. Chem. Bull.* **2013**, *62*, 2477.

(28) Leach, A. G.; Houk, K. N. Transition States and Mechanisms of the Hetero-Diels-Alder Reactions of Hyponitrous Acid, Nitrosoalkanes, Nitrosoarenes, and Nitrosocarbonyl Compounds. *J. Org. Chem.* **2001**, *66*, 5192.

(29) Thomas, S. P.; French, R. M.; Jheengut, V.; Aggarwal, V. K. Homologation and Alkylation of Boronic Esters and Boranes by 1,2-Metallate Rearrangement of Boron Ate Complexes. *Chem. Rec.* **2009**, *9*, 24.

(30) For analogous calculations using a PCM model for solvation in *n*-butyl acetate (ε = 4.9941), see ref 15c.

(31) Ono, N. *The Nitro Group in Organic Synthesis*; Wiley: New York, 2001.

(32) Srivastava, R. S.; Nicholas, K. M. Kinetics of the Allylic Amination of Olefins by Nitroarenes Catalyzed by $[CpFe(CO)_2]_2$. *Organometallics* **2005**, *24*, 1563.

(33) Gui, J.; Pan, C.-M.; Jin, Y.; Qin, T.; Lo, J. C.; Lee, B. J.; Spergel, S. H.; Mertzman, M. E.; Pitts, W. J.; La Cruz, T. E.; Schmidt, M. A.; Darvatkar, N.; Natarajan, S. R.; Baran, P. S. Practical olefin hydroamination with nitroarenes. *Science* **2015**, *348*, 886.

(34) Zhu, K.; Shaver, M. P.; Thomas, S. P. Chemoselective Nitro Reduction and Hydroamination Using a Single Iron Catalyst. *Chem. Sci.* **2016**, *7*, 3031.

(35) (a) Cheung, C. W.; Hu, X. Amine Synthesis via Iron-Catalysed Reductive Coupling of Nitroarenes with Alkyl Halides. *Nat. Commun.* **2016**, *7*, 12494. (b) Cheung, C. W.; Ploeger, M. L.; Hu, X. Direct Amidation of Esters with Nitroarenes. *Nat. Commun.* **2017**, *8*, 14878. (c) Cheung, C. W.; Ploeger, M. L.; Hu, X. Nickel-Catalyzed Reductive Transamidation of Secondary Amides with Nitroarenes. *ACS Catal.* **2017**, *7*, 7092.

(36) (a) Sapountzis, I.; Knochel, P. A New General Preparation of Polyfunctional Diarylamines by the Addition of Functionalized Arylmagnesium Compounds to Nitroarenes. *J. Am. Chem. Soc.* **2002**, *124*, 9390. (b) Dohle, W.; Staubitz, A.; Knochel, P. Mild Synthesis of Polyfunctional Benzimidazoles and Indoles by the Reduction of Functionalized Nitroarenes with Phenylmagnesium Chloride. *Chem. - Eur. J.* **2003**, *9*, 5323. (c) Kopp, F.; Sapountzis, I.; Knochel, P. Preparation of Polyfunctionalized Amines by the Addition of Functionalized Organomagnesium Reagents to Nitrosoarenes. *Synlett* **2003**, 885. (d) Sapountzis, I.; Knochel, P. A New Method for the Selective Amination of 1,3- and 1,4-Dinitrobenzenes and Protected Nitroanilines Leading to Polyfunctional 1,3- and 1,4-Disubstituted Anilines. *Synlett* **2004**, 955. (e) Dhayalan, V.; Saemann, C.; Knochel, P. Synthesis of polyfunctional secondary amines by the addition of functionalized zinc reagents to nitrosoarenes. *Chem. Commun.* **2015**, *51*, 3239.

(37) Gao, H.; Xu, Q.-L.; Yousufuddin, M.; Ess, D. H.; Kurti, L. Transition-Metal-Free, Low-Temperature Intramolecular Amination of Aromatic C-H Bonds: Rapid Synthesis of Fused Heterocycles. *Angew. Chem., Int. Ed.* **2014**, *53*, 2701.

(38) (a) Rauser, M.; Ascheberg, C.; Niggemann, M. Electrophilic Amination with Nitroarenes. *Angew. Chem., Int. Ed.* **2017**, *56*, 11570. (b) Rauser, M.; Ascheberg, C.; Niggemann, M. Direct Reductive N-Functionalization of Aliphatic Nitro Compounds. *Chem. - Eur. J.* **2018**, *24*, 3970. (c) Rauser, M.; Warzecha, D. P.; Niggemann, M. O_2-Mediated Oxidation of Aminoboranes through 1,2-N Migration. *Angew. Chem., Int. Ed.* **2018**, *57*, 5903. (d) Rauser, M.; Eckert, R.; Gerbershagen, M.; Niggemann, M. Catalyst-Free Reductive Coupling of Aromatic and Aliphatic Nitro Compounds with Organohalides. *Angew. Chem., Int. Ed.* **2019**, *58*, 6713.

(39) Nykaza, T. V.; Yang, J.; Radosevich, A. T. PEt₃-Mediated Deoxygenative C−N Coupling of Nitroarenes and Boronic Acids. *Tetrahedron* **2019**, *75*, 3248.

(40) Roscales, S.; Csáky, A. G. Transition-Metal-Free Three-Component Synthesis of Tertiary Aryl Amines from Nitro Compounds, Boronic Acids, and Trialkyl Phosphites. *Adv. Synth. Catal.* **2020**, *362*, 111.

(41) Suárez-Pantiga, S.; Hernández-Ruiz, R.; Virumbrales, C.; Pedrosa, M. R.; Sanz, R. Reductive Molybdenum-Catalyzed Direct Amination of Boronic Acids with Nitro Compounds. *Angew. Chem., Int. Ed.* **2019**, *58*, 2129.

(42) O'Brien, C. J.; Tellez, J. L.; Nixon, Z. S.; Kang, L. J.; Carter, A. L.; Kunkel, S. R.; Przeworski, K. C.; Chass, G. A. Recycling the Waste: The Development of a Catalytic Wittig Reaction. *Angew. Chem., Int. Ed.* **2009**, *48*, 6836.

(43) (a) O'Brien, C. J.; Lavigne, F.; Coyle, E. E.; Holohan, A. J.; Doonan, B. J. Breaking the ring through a room temperature catalytic Wittig reaction. *Chem. - Eur. J.* **2013**, *19*, 5854. (b) O'Brien, C. J.; Nixon, Z. S.; Holohan, A. J.; Kunkel, S. R.; Tellez, J. L.; Doonan, B. J.; Coyle, E. E.; Lavigne, F.; Kang, L. J.; Przeworski, K. C. The development of the catalytic Wittig reaction. *Chem. - Eur. J.* **2013**, *19*, 15281. (c) Coyle, E. E.; Doonan, B. J.; Holohan, A. J.; Walsh, K. A.; Lavigne, F.; Krenske, E. H.; O'Brien, C. J. Catalytic Wittig reactions of semi-and nonstabilized ylides enabled by ylide tuning. *Angew. Chem., Int. Ed.* **2014**, *53*, 12907. (d) Kirk, A. M.; O'Brien, C. J.; Krenske, E. H. Why Do Silanes Reduce Electron-Rich Phosphine Oxides Faster than Electron-Poor Phosphine Oxides? *Chem. Commun.* **2020**, *56*, 1227.

(44) (a) Guo, H.; Fan, Y. C.; Sun, Z.; Wu, Y.; Kwon, O. Phosphine Organocatalysis. *Chem. Rev.* **2018**, *118*, 10049. (b) Lao, Z.; Toy, P. H. Catalytic Wittig and aza-Wittig Reactions. *Beilstein J. Org. Chem.* **2016**, *12*, 2577.

(45) For reviews discussing P^V=O catalysis, see: (a) Marsden, S. P. Catalytic Variants of Phosphine Oxide-Mediated Organic Transformations. In *Sustainable Catalysis*; Dunn, P. J., Hii, K. K., Krische, M. J., Williams, M. T., Eds.; John Wiley & Sons, Inc.: New York, 2013; pp 339−361. (b) Denmark, S. E.; Stavenger, R. A. Asymmetric Catalysis of Aldol Reactions with Chiral Lewis Bases. *Acc. Chem. Res.* **2000**, *33*, 432. (c) Denmark, S. E.; Beutner, G. L. Lewis Base Catalysis in Organic Synthesis. *Angew. Chem., Int. Ed.* **2008**, *47*, 1560. (d) Benaglia, M.; Rossi, S. Chiral Phosphine Oxides in Present-Day Organocatalysis. *Org. Biomol. Chem.* **2010**, *8*, 3824.

(46) (a) Denton, R. M.; An, J.; Adeniran, B. Phosphine Oxide-Catalysed Chlorination Reactions of Alcohols Under Appel Conditions. *Chem. Commun.* **2010**, *46*, 3025. (b) Denton, R. M.; Tang, X.; Przeslak, A. Catalysis of Phosphorus(V)-Mediated Transformations: Dichlorination Reactions of Epoxides Under Appel Conditions. *Org. Lett.* **2010**, *12*, 4678. (c) Denton, R. M.; An, J.; Adeniran, B.; Blake, A. J.; Lewis, W.; Poulton, A. M. Catalytic Phosphorus(V)-Mediated Nucleophilic Substitution Reactions: Development of a Catalytic Appel Reaction. *J. Org. Chem.* **2011**, *76*, 6749. (d) An, J.; Tang, X.; Moore, J.; Lewis, W.; Denton, R. M. Phosphorus(V)-Catalyzed Deoxydichlorination Reactions of Aldehydes. *Tetrahedron* **2013**, *69*, 8769. (e) Yu, T.-Y.; Wang, Y.; Xu, P.-F. An Unusual Triphenylphosphine Oxide Catalyzed Stereoselective 1,3-Dichlorination of Unsaturated Ketoesters. *Chem. - Eur. J.* **2014**, *20*, 98. (f) Tang, X.; An, J.; Denton, R. M. A Procedure for Appel Halogenations and Dehydrations Using a Polystyrene Supported Phosphine Oxide. *Tetrahedron Lett.* **2014**, *55*, 799. (g) Buonomo, J. A.; Aldrich, C. C. Mitsunobu Reactions Catalytic in Phosphine and a Fully Catalytic System. *Angew. Chem., Int. Ed.* **2015**, *54*, 13041. (h) Hirose, D.; Gazvoda, M.; Košmrlj, J.; Taniguchi, T. The "Fully Catalytic System" in Mitsunobu Reaction Has Not Been Realized Yet. *Org. Lett.* **2016**, *18*, 4036. (i) Jiang, L.; Yu, J.; Niu, F.; Zhang, D.; Sun, X. A High-Efficient Method for the Amidation of Carboxylic Acids Promoted by Triphenylphosphine Oxide and Oxalyl Chloride. *Heteroat. Chem.* **2017**, *28*, No. e21364. (j) Beddoe, R. H.; Sneddon, H. F.; Denton, R. M. The Catalytic Mitsunobu Reaction: A Critical Analysis of the Current State-of-the-Art. *Org. Biomol. Chem.* **2018**, *16*, 7774. (k) Beddoe, R. H.; Andrews, K. G.; Magné, V.; Cuthbertson, J. D.; Saska, J.; Shannon-Little, A. L.; Shanahan, S. E.; Sneddon, H. F.; Denton, R. M. Redox-Neutral Organocatalytic Mitsunobu Reactions. *Science* **2019**, *365*, 910.

(47) Harris, J. R.; Haynes, M. T., II; Thomas, A. M.; Woerpel, K. A. Phosphine-catalyzed reductions of alkyl silyl peroxides by titanium hydride reducing agents: Development of the method and mechanistic investigations. *J. Org. Chem.* **2010**, *75*, 5083.

(48) (a) van Kalkeren, H. A.; van Delft, F. L.; Rutjes, F. P. J. T. Organophosphorus catalysis to bypass phosphine oxide waste. *ChemSusChem* **2013**, *6*, 1615. (b) van Kalkeren, H. A.; Blom, A. L.; Rutjes, F. P. J. T.; Huijbregts, M. A. J. On the usefulness of life cycle assessment in early chemical methodology development: The case of organophosphorus-catalyzed Appel and Wittig reactions. *Green Chem.* **2013**, *15*, 1255. (c) van Kalkeren, H. A.; Leenders, S. H.; Hommersom, C. R.; Rutjes, F. P.; van Delft, F. L. In situ phosphine oxide reduction: A catalytic Appel reaction. *Chem. - Eur. J.* **2011**, *17*, 11290. (d) van Kalkeren, H. A.; van Delft, F. L.; Rutjes, F. P. J. T. Catalytic Appel reactions. *Pure Appl. Chem.* **2012**, *85*, 817. (e) van Kalkeren, H. A.; Bruins, J. J.; Rutjes, F. P. J. T.; van Delft, F. L. Organophosphorus-catalysed Staudinger reduction. *Adv. Synth. Catal.* **2012**, *354*, 1417. (f) van Kalkeren, H. A.; te Grotenhuis, C.; Haasjes, F. S.; Hommersom, C. R. A.; Rutjes, F. P. J. T.; van Delft, F. L. Catalytic Staudinger/aza-Wittig sequence by in situ phosphane oxide. *Eur. J. Org. Chem.* **2013**, *2013*, 7059. (g) Lenstra, D. C.; Rutjes, F. P.; Mecinović, J. Triphenylphosphine catalysed amide bond formation between carboxylic acids and amines. *Chem. Commun.* **2014**, *50*, 5763.

(49) (a) Werner, T. Phosphonium salt organocatalysis. *Adv. Synth. Catal.* **2009**, *351*, 1469. (b) Werner, T.; Hoffmann, M.; Deshmukh, S. First enantioselective catalytic Wittig reaction. *Eur. J. Org. Chem.* **2014**, *2014*, 6630. (c) Werner, T.; Hoffmann, M.; Deshmukh, S. First microwaveassisted catalytic Wittig reaction. *Eur. J. Org. Chem.* **2014**, *2014*, 6873. (d) Hoffmann, M.; Deshmukh, S.; Werner, T. Scope and limitation of the microwave-assisted catalytic Wittig reaction. *Eur. J. Org. Chem.* **2015**, *2015*, 4532. (e) Werner, T.; Hoffmann, M.; Deshmukh, S. Phospholane catalyzed Wittig reaction. *Eur. J. Org. Chem.* **2015**, *2015*, 3286. (f) Schirmer, M. L.; Adomeit, S.; Werner, T. First base-free catalytic Wittig reaction. *Org. Lett.* **2015**, *17*, 3078. (g) Schirmer, M. L.; Adomeit, S.; Spannenberg, A.; Werner, T. Novel base-free catalytic Wittig reaction for the synthesis of highly functionalized alkenes. *Chem. - Eur. J.* **2016**, *22*, 2458. (h) Longwitz, L.; Spannenberg, A.; Werner, T. Phosphetane Oxides as Redox Cycling Catalysts in the Catalytic Wittig Reaction at Room Temperature. *ACS Catal.* **2019**, *9*, 9237. (i) Longwitz, L.; Werner, T. Reduction of Activated Alkenes by P$^{(III)}$/P$^{(V)}$ Redox Cycling Catalysis. *Angew. Chem., Int. Ed.* **2020**, *59*, 2760.

(50) (a) Zhang, K.; Cai, L.; Yang, Z.; Houk, K. N.; Kwon, O. Bridged [2.2.1] bicyclic phosphine oxide facilitates catalytic γ-umpolung addition-Wittig olefination. *Chem. Sci.* **2018**, *9*, 1867. (b) Cai, L.; Zhang, K.; Chen, S.; Lepage, R. J.; Houk, K. N.; Krenske, E. H.; Kwon, O. Catalytic Asymmetric Staudinger-Aza-Wittig Reaction for the Synthesis of Heterocyclic Amines. *J. Am. Chem. Soc.* **2019**, *141*, 9537.

(51) (a) Fourmy, K.; Voituriez, A. Catalytic cyclization reactions of Huisgen zwitterion with α-ketoesters by in situ chemoselective phosphine oxide reduction. *Org. Lett.* **2015**, *17*, 1537. (b) Saleh, N.; Voituriez, A. Synthesis of 9*H*-pyrrolo[1,2-*a*]indole and 3*H*-pyrrolizine derivatives via a phosphine-catalyzed umpolung addition/intramolecular Wittig reaction. *J. Org. Chem.* **2016**, *81*, 4371. (c) Saleh, N.; Blanchard, F.; Voituriez, A. Synthesis of nitrogencontaining heterocycles and cyclopentenone derivatives via phosphinecatalyzed Michael addition/intramolecular Wittig reaction. *Adv. Synth. Catal.* **2017**, *359*, 2304.

(52) (a) Tsai, Y.-L.; Lin, W. Synthesis of multifunctional alkenes from substituted acrylates and aldehydes via phosphine-catalyzed Wittig reaction. *Asian J. Org. Chem.* **2015**, *4*, 1040. (b) Lee, C.; Chang, T.; Yu, J.; Reddy, G. M.; Hsiao, M.; Lin, W. Synthesis of Functionalized Furans via Chemoselective Reduction/Wittig Reaction Using Catalytic Triethylamine and Phosphine. *Org. Lett.* **2016**, *18*, 3758.

(53) (a) Wang, L.; Sun, M.; Ding, M.-W. Catalytic intramolecular Wittig reaction based on a phosphine/phosphine oxide catalytic cycle for the synthesis of heterocycles. *Eur. J. Org. Chem.* **2017**, *2017*, 2568.

(b) Wang, L.; Wang, Y.; Chen, M.; Ding, M.-W. Reversible P$^{(III)}$/P$^{(V)}$ redox: Catalytic aza-Wittig reaction for the synthesis of 4(3*H*)-quinazolinones and the natural product vasicinone. *Adv. Synth. Catal.* **2014**, *356*, 1098. (c) Wang, L.; Xie, Y.-B.; Huang, N.-Y.; Yan, J.-Y.; Hu, W.-M.; Liu, M.-G.; Ding, M.-W. Catalytic aza-Wittig reaction of acid anhydride for the synthesis of 4*H*-benzo[*d*][1,3]oxazin-4-ones and 4-benzylidene-2- aryloxazol-5(4*H*)-ones. *ACS Catal.* **2016**, *6*, 4010.

(54) Rommel, S.; Belger, C.; Begouin, J.; Plietker, B. Dual [Fe + Phosphine] catalysis: Application in catalytic Wittig olefination. *ChemCatChem* **2015**, *7*, 1292.

(55) Bel Abed, H.; Mammoliti, O.; Bande, O.; Van Lommen, G.; Herdewijn, P. Organophosphorus-catalyzed diaza-Wittig reaction: Application to the synthesis of pyridazines. *Org. Biomol. Chem.* **2014**, *12*, 7159.

(56) (a) Marsi, K. L. Stereochemistry of Some Reactions of Phospholane Derivatives. *J. Am. Chem. Soc.* **1969**, *91*, 4724. (b) Marsi, K. L. Phenylsilane Reduction of Phosphine Oxides with Complete Stereospecificity. *J. Org. Chem.* **1974**, *39*, 265.

(57) Keglevich, G.; Fekete, M.; Chuluunbaatar, T.; Dobo, A.; Harmat, V.; Toke, L. One-pot Transformation of Cyclic Phosphine Oxides to Phosphine—Boranes by Dimethyl Sulfide—borane. *J. Chem. Soc., Perkin Trans.* **2000**, *1*, 4451.

(58) (a) Cadogan, J. I. G.; Cameron-Wood, M.; Mackie, R. K.; Searle, R. J. G. The Reactivity of Organophosphorus Compounds. Part XIX. Reduction of Nitro-Compounds by Triethyl Phosphite: A Convenient New Route to Carbazoles, Indoles, Indazoles, Triazoles, and Related Compounds. *J. Chem. Soc.* **1965**, *0*, 4831. (b) Cadogan, J. I. G. Reduction of Nitro- and Nitroso-Compounds by Tervalent Phosphorus Reagents. *Q. Rev., Chem. Soc.* **1968**, *22*, 222. (c) Cadogan, J. I. G.; Todd, M. J. Reduction of Nitro- and Nitroso-Compounds by Tervalent Phosphorus Reagents. Part IV. Mechanistic Aspects of the Reduction of 2,4,6-Trimethyl-2'-Nitrobiphenyl, 2-Nitrobiphenyl, and Nitrobenzene. *J. Chem. Soc. C* **1969**, *0*, 2808. (d) Armour, M. A.; Cadogan, J. I. G.; Grace, D. S. B. Reduction of Nitro- and Nitroso-Compounds by Tervalent Phosphorus Reagents. Part XI. A Kinetic Study of the Effects of Varying the Reagent and the Nitro-Compound in the Conversion of o-Nitrobenzylideneamines to 2-Substituted Indazoles. *J. Chem. Soc., Perkin Trans. 2* **1975**, *2* (11), 1185.

(59) Sundberg, R. J.; Lang, C.-C. Structure-reactivity Studies of Deoxygenation Reactions. *J. Org. Chem.* **1971**, *36*, 300.

(60) For amination reactions with more Lewis acidic organoboron reagents, see (a) Brown, H. C.; Salunkhe, A. M.; Singaram, B. Chiral Synthesis via Organoboranes. 28. Reaction of α-Chiral Organyldichloroboranes with Organyl Azides Providing a Synthesis of Secondary Amines with Exceptionally High Enantiomeric Purities. *J. Org. Chem.* **1991**, *56*, 1170. (b) Phanstiel, O., IV; Wang, Q. X.; Powell, D. H.; Ospina, M. P.; Leeson, B. A. Synthesis of Secondary Amines via N-(Benzoyloxy)Amines and Organoboranes. *J. Org. Chem.* **1999**, *64*, 803. (c) Kim, B. J.; Matteson, D. S. Conversion of Alkyltrifluoroborates into Alkyldichloroboranes with Tetrachlorosilane in Coordinating Solvents. *Angew. Chem., Int. Ed.* **2004**, *43*, 3056. (d) Ou, L.; Shao, J.; Zhang, G.; Yu, Y. Metal-Free Carbon-Nitrogen Bond-Forming Coupling Reaction between Arylboronic Acids and Organic Azides. *Tetrahedron Lett.* **2011**, *52*, 1430.

(61) For amination reactions with boronic acids, see: (a) Zhu, C.; Li, G.; Ess, D. H.; Falck, J. R.; Kürti, L. Elusive Metal-Free Primary Amination of Arylboronic Acids: Synthetic Studies and Mechanism by Density Functional Theory. *J. Am. Chem. Soc.* **2012**, *134*, 18253. (b) Coeffard, V.; Moreau, X.; Thomassigny, C.; Greck, C. Transition-Metal-Free Amination of Aryl Boronic Acids and Their Derivatives. *Angew. Chem., Int. Ed.* **2013**, *52*, 5684. (c) Voth, S.; Hollett, J. W.; Mccubbin, J. A. Transition-Metal-Free Access to Primary Anilines from Boronic Acids and a Common $^+$NH$_2$ Equivalent. *J. Org. Chem.* **2015**, *80*, 2545. (d) Sun, H.; Gong, L.; Tian, Y.; Wu, J.; Zhang, X.; Liu, J.; Fu, Z.; Niu, D. Metal- and Base-Free Room-Temperature Amination of Organoboronic Acids with N-Alkyl Hydroxylamines. *Angew. Chem., Int. Ed.* **2018**, *57*, 9456.

(62) Starkov, P.; Jamison, T. F.; Marek, I. Electrophilic Amination: The case of Nitrenoids. *Chem. - Eur. J.* **2015**, *21*, 5278.

(63) Lower oxygenates of nitrogen or alternative nitrogen reagents are more common in C−N bond formation with boronic acids. Nitrosoarenes: (a) Yu, Y.; Srogl, J.; Liebeskind, L. S. Cu(I)-Mediated Reductive Amination of Boronic Acids with Nitroso Aromatics. *Org. Lett.* **2004**, *6*, 2631. (b) Roscales, S.; Csákÿ, A. G. Synthesis of Di(hetero)arylamines from Nitrosoarenes and Boronic Acids: A General, Mild, and Transition-Metal-Free Coupling. *Org. Lett.* **2018**, *20*, 1667. *N*-Alkyl hydroxylamines: (c) Sarma, M. J.; Phukan, P. Metal-Free Synthesis of Secondary Amines by the Reaction of Tosyl Triazene and Aryl Boronic Acid. *Synth. Commun.* **2018**, *48*, 656.

(64) Accurate reaction sampling and dilution was performed using a probe-based Mettler-Toledo EasySampler 1210 system, see: Zawatzky, K.; Grosser, S.; Welch, C. J. Facile Kinetic Profiling of Chemical Reactions Using MISER Chromatographic Analysis. *Tetrahedron* **2017**, *73*, 5048.

(65) Frisch, M. J.; Trucks, G. W.; Schlegel, H. B.; Scuseria, G. E.; Robb, M. A.; Cheeseman, J. R.; Scalmani, G.; Barone, V.; Mennucci, B.; Petersson, G. A.; Nakatsuji, H.; Caricato, M.; Li, X.; Hratchian, H. P.; Izmaylov, A. F.; Bloino, J.; Zheng, G.; Sonnenberg, J. L.; Hada, M.; Ehara, M.; Toyota, K.; Fukuda, R.; Hasegawa, J.; Ishida, M.; Nakajima, T.; Honda, Y.; Kitao, O.; Nakai, H.; Vreven, T.; Montgomery, J. A., Jr.; Peralta, J. E.; Ogliaro, F.; Bearpark, M.; Heyd, J. J.; Brothers, E.; Kudin, K. N.; Staroverov, V. N.; Kobayashi, R.; Normand, J.; Raghavachari, K.; Rendell, A.; Burant, J. C.; Iyengar, S. S.; Tomasi, J.; Cossi, M.; Rega, N.; Millam, N. J.; Klene, M.; Knox, J. E.; Cross, J. B.; Bakken, V.; Adamo, C.; Jaramillo, J.; Gomperts, R.; Stratmann, R. E.; Yazyev, O.; Austin, A. J.; Cammi, R.; Pomelli, C.; Ochterski, J. W.; Martin, R. L.; Morokuma, K.; Zakrzewski, V. G.; Voth, G. A.; Salvador, P.; Dannenberg, J. J.; Dapprich, S.; Daniels, A. D.; Farkas, Ö.; Foresman, J. B.; Ortiz, J. V.; Cioslowski, J.; Fox, D. J. *Gaussian 09*, revision B.01; Gaussian, Inc.: Wallingford, CT, 2009.

(66) (a) Zhao, Y.; Truhlar, D. G. The M06 Suite of Density Functionals for Main Group Thermochemistry, Thermochemical Kinetics, Noncovalent Interactions, Excited States, and Transition Elements: two New Functionals and Systematic Testing of four M06-class Functionals and 12 Other Functionals. *Theor. Chem. Acc.* **2008**, *120*, 215. (b) Zhao, Y.; Truhlar, D. G. Density Functionals with Broad Applicability in Chemistry. *Acc. Chem. Res.* **2008**, *41*, 157.

(67) Yamaguchi, K.; Takahara, Y.; Fueno, T.; Houk, K. N. Extended Hartree-Fock (EHF) Theory of Chemical Reactions - III. Projected Møller-Plesset (PMP) Perturbation Wavefunctions for Transition Structures of Organic Reactions. *Theor. Chim. Acta* **1988**, *73*, 337.